

University of Louisville

ThinkIR: The University of Louisville's Institutional Repository

Electronic Theses and Dissertations

8-2021

Development of 3D-bioprinted scaffolds for oral probiotic application.

Jhanvi Patel
University of Louisville

Follow this and additional works at: <https://ir.library.louisville.edu/etd>



Part of the [Oral Biology and Oral Pathology Commons](#)

Recommended Citation

Patel, Jhanvi, "Development of 3D-bioprinted scaffolds for oral probiotic application." (2021). *Electronic Theses and Dissertations*. Paper 4249.

<https://doi.org/10.18297/etd/4249>

This Master's Thesis is brought to you for free and open access by ThinkIR: The University of Louisville's Institutional Repository. It has been accepted for inclusion in Electronic Theses and Dissertations by an authorized administrator of ThinkIR: The University of Louisville's Institutional Repository. This title appears here courtesy of the author, who has retained all other copyrights. For more information, please contact thinkir@louisville.edu.

DEVELOPMENT OF 3D-BIOPRINTED SCAFFOLDS FOR
ORAL PROBIOTIC APPLICATION

By
Jhanvi Patel

B.D.S., College of Dental Sciences and Research Centre,
Gujarat, India 2016

A Thesis
Submitted to the Faculty of the
School of Dentistry of the University of Louisville
in Partial Fulfillment of the Requirements
for the Degree of

Master of Science
in Oral Biology

Department of Oral Immunology and Infectious Disease
School of Dentistry
University of Louisville
Louisville, KY

August 2021

Copyright 2021 by Jhanvi Patel
All Rights Reserved

DEVELOPMENT OF 3D-BIOPRINTED SCAFFOLDS FOR
ORAL PROBIOTIC APPLICATION

By
Jhanvi Patel
B.D.S., College of Dental Sciences and Research Centre,
Gujarat, India 2016

Thesis Approved on

July 8th 2021

By the following Thesis Committee:

Dr. Jill M. Steinbach-Rankins, Ph.D.
Thesis Director

Dr. Donald R. Demuth, Ph.D.
Co-Mentor

Dr. David A. Scott, Ph.D.

Dr. Michele M. Pisano, Ph.D.

DEDICATION

This thesis is dedicated to
My parents Dr. Kanaiyal and Pushpaben Patel,
Husband Hem Patel,
Family Kalpeshbhai, Sarikaben, Kautilya, Prima, Hardika Patel
For encouraging me to achieve my goals and supporting me
throughout my journey.

ACKNOWLEDGMENT

I would like to sincerely thank my mentors Dr. Jill M. Steinbach-Rankins and Dr. Donald R. Demuth for providing me an opportunity to be part of their lab and constantly helping me with my research project. I highly appreciate your guidance and continuous efforts to make this project a success. I am also thankful to Dr. Michele M. Pisano, Director of my master's program and thesis committee member, for her tremendous encouragement and directions to help me grow professionally and personally. I also wish to thank Dr. David A. Scott for his guidance as a committee member and support during my research work. Finally, I am thankful to Jinlian Tan and Kiel Butterfield for assisting me throughout my research work.

ABSTRACT

DEVELOPMENT OF 3D-BIOPRINTED SCAFFOLDS FOR ORAL APPLICATIONS OF PROBIOTICS

Jhanvi Patel

June 08, 2021

Background: *Porphyromonas gingivalis* adheres to and invades gingival epithelial cells, resulting in decreased cell viability. Previous studies have indicated that probiotics are effective against dental pathogens; however, few approaches provide sustained-delivery of active agents in the oral cavity.

Hypothesis: Probiotics will limit *P. gingivalis* effects on Telomerase Immortalized Gingival Keratinocyte (TIGK) cells and 3D-printed scaffolds will prolong probiotic release.

Methods: *Lactobacillus acidophilus*, *Lactobacillus reuteri*, and *Bifidobacterium bifidum* were assessed with adhesion and antibiotic protection assays to limit *P. gingivalis* effects on TIGKs. Scaffolds were printed with a select probiotic and evaluated for release kinetics.

Results: Free *L.a.*, *L.r.*, and *B.b.* administration improved TIGK viability by reducing *P. gingivalis* adhesion. Additionally, probiotic-containing scaffolds were successfully printed, demonstrating high viability and sustained-release of probiotics over two weeks.

Conclusion: Probiotics effectively limit *P. gingivalis* adhesion to TIGKs, suggesting that 3D-bioprinted probiotic-containing scaffolds may be a promising delivery system for mitigating *P. gingivalis* colonization.

TABLE OF CONTENTS

ACKNOWLEDGEMENT.....	iv
ABSTRACT.....	v
CHAPTER 1.....	1
INTRODUCTION.....	1
CHAPTER 2.....	23
HYPOTHESIS AND SPECIFIC AIMS.....	23
CHAPTER 3.....	24
MATERIALS AND METHODS.....	24
CHAPTER 4.....	33
RESULTS.....	33
CHAPTER 5.....	47
DISCUSSION.....	47
REFERENCES.....	53
CURRICULUM VITAE.....	61

LIST OF FIGURES

Page

<u>Figure 1:</u> Schematic representation of <i>P. gingivalis</i> determinant involved in adhesion to oral structures and fimbriae FimA and Mfa1 interactions with epithelial cells and other bacteria.....	6
<u>Figure 2:</u> Image showing adhesion and invasion of <i>P. gingivalis</i> to gingival epithelial cells	7
<u>Figure 3:</u> Schematic of potential mechanism of probiotics to confer health benefits to host.....	12
<u>Figure 4:</u> Different bacterial genera classified under probiotics category.....	13
<u>Figure 5:</u> Schematic representation of stepwise procedure for 3D-bioprinting.....	18
<u>Figure 6:</u> Illustration of different categories of bioinks.....	19
<u>Figure 7:</u> Schematic representation of different bioprinting techniques.....	22
<u>Figure 8:</u> Schematic representation for adhesion assay.....	26
<u>Figure 9:</u> Overview of antibiotic protection assay.....	27
<u>Figure 10:</u> Allevi 3 bioprinter with three extruders.....	30
<u>Figure 11:</u> Overview of steps involved to determine post-printing viability.....	31
<u>Figure 12:</u> A brief illustration of release assay procedure.....	32

<u>Figure 13:</u> Determination of CS and HI-labeled <i>P. gingivalis</i> adhesion efficacy to TIGK cells.....	34
<u>Figure 14:</u> <i>P. gingivalis</i> binding to TIGKs after <i>Lactobacillus acidophilus</i> pre- or co-treatment.....	35
<u>Figure 15:</u> <i>P. gingivalis</i> binding to TIGKs after <i>Lactobacillus reuteri</i> pre- or co-treatment.....	37
<u>Figure 16:</u> <i>P. gingivalis</i> binding to TIGKs after <i>Bifidobacterium bifidum</i> pre- or co-treatment.....	39
<u>Figure 17:</u> <i>P. gingivalis</i> invasion of TIGKs.....	40
<u>Figure 18:</u> Comparison of LDH secretion from unlysed and lysed TIGKs at different cell densities.....	42
<u>Figure 19:</u> Evaluation of LDH expression after administration of different MOIs of <i>P. gingivalis</i>	43
<u>Figure 20:</u> Different morphology of 3D-bioprinted scaffolds.....	44
<u>Figure 21:</u> Probiotic viability pre- and post-printing after initial incorporation of 5×10^7 CFU <i>Lactobacillus acidophilus</i> per mg of scaffold.....	45
<u>Figure 22:</u> Cumulative release of <i>Lactobacillus acidophilus</i> from 3D-printed scaffolds in PBS, MRS broth, and artificial saliva.....	46

CHAPTER 1
INTRODUCTION

Prevalence and Impact of Periodontitis

Among currently prevalent oral diseases, biofilm-mediated periodontitis has become the major concern for oral health. Periodontitis, expressed as a chronic inflammation of tooth supporting structure, begins as gingivitis and progresses into severe destruction of periodontal ligament, alveolar bone, and eventually tooth loss. Periodontal diseases are the major cause of tooth loss in adults older than 30 years. However, threats associated with periodontal disease are not limited to oral health but are also linked with lethal systemic diseases such as osteoporosis, type 2 diabetes mellitus, cardiovascular diseases and rheumatoid arthritis, as well as abnormal pregnancy outcomes such as low birth weights and premature labor [1]. The National Health and Nutritional Examination survey identified 46% of U.S. adults aged 30 years or older to be suffering from periodontitis, representing roughly 141 million adult Americans. Among these, 8.9% of affected individuals suffer from advanced periodontal disease, which involves severe destruction of tooth supporting periodontium [2] and these numbers are expected to rise. Reports indicate that the estimated global cost of direct treatment for oral diseases, including periodontitis, was US \$298 billion – accounting for approximately 4.6% of the total money spent on global health [3]. Unfortunately, many people affected by periodontitis are unable to afford treatment, with ~538 million people living with untreated periodontal disease [4].

Oral Manifestations of Periodontitis

Clinically, periodontitis is expressed from a milder form of gingivitis to a more advanced and correspondingly destructive form of chronic periodontitis. Periodontitis begins as gingivitis that is caused by subgingival formation of a biofilm. Gingivitis is demarcated through the clinical signs of inflammation, bleeding on gentle probing, promoting discomfort, and progressing plaque formation [5]. At this stage,

gingivitis is a reversible disease, which can be resolved by supra- and subgingival plaque elimination through mechanical maneuvering like scaling and root planing. However, if left untreated, gingivitis combined with poor oral health care can progress to periodontitis. Periodontitis is clinically expressed as a chronic inflammatory response that progresses to the destruction of connective tissue, resorption of tooth supporting alveolar bone, mobility and ultimately the loosening and loss of teeth [5]. Diagnosis of chronic periodontitis is based on clinical and radiographic assessment of the subgingival clinical attachment loss (≥ 5 mm), bleeding on probing, and bone loss [5]. Chronic periodontitis causes irreversible tissue damage that requires diligent protective care and maintenance of oral hygiene to prevent recurrence [6].

Biofilm Formation and Role in Periodontitis

Periodontal disease is a biofilm-mediated inflammatory disease. Therefore, a thorough understanding of biofilm formation, properties, and mechanism of disease progression will assist in developing effective therapies to prevent and treat periodontal disease. Biofilms are formed of a conglomerate of organisms embedded in a matrix containing extracellular polymeric substances. As the bacterial colonies in the biofilm grow, the biofilm develops “emergent properties” that protect the biofilm and impart biofilm resilience against environmental changes [7]. However, when environmental alterations exceed a threshold, the overgrowth of certain microorganisms in the biofilm is initiated, leading to disruption in host homeostasis and dysbiosis [8].

Biofilm formation and maturation are categorized in three different stages, which result in a structured and functionally well-organized microbial community.

(1) Initial adhesion to tooth surface

The first step in the development of dental plaque (or biofilms) is the formation of a thin coating of acquired pellicle on the tooth enamel. This coating is mainly comprised of proteins and other macromolecules such as albumin, proline-rich proteins, glycoproteins, sialic acids, and alpha amylase, which are absorbed from saliva and gingival crevicular fluid [8, 9]. Streptococci, considered as 80% of primary colonizers, bind to this pellicle by adhesins, such as antigen I/II protein family, and serine-rich glycoproteins [10-13]. In addition to

streptococci, *Actinomyces oris* also colonizes via type 1 fimbria to proline rich protein (PRPs) and pellicle statherin [14]. This initial colonization is an important step for plaque development as it prevents bacteria washing by saliva and provides a surface for subsequent bacterial adhesion [15].

(2) Bacterial coaggregation and biofilm maturation

The second stage of biofilm development involves the adhesion of secondary colonizers to previously attached bacterial cells and resulting biofilm maturation [15, 16]. The interspecies interactions between these secondary bacteria with previously colonized bacteria are known as coaggregation, which leads to an increase in biofilm biomass [17]. Bacterial coaggregation initiates bacterial co-localization of physiologically relevant organisms in the same milieu, which leads to cell-cell signalling, development of complex nutritional systems, and gene transfer [8]. This type of complex microbial community is interdependent for nutrition where the metabolic byproduct of one species becomes the nutrient source of another species, thereby directing the order of colonization [18]. It forms a functionally-structured community by colonizing bacteria according to specific metabolic pathways [18]. Signalling mechanism between cells facilitate bacterial cells to control the expression of virulence-regulating genes and adapt to environmental stimuli [8]. Additionally, the proximity of cells also allows horizontal gene transfer, which increases the adaptive ability of the organisms to alter oral environmental factors [19]. As the biofilm becomes more structured, organisms within the biofilm alter gene expression to form a viscous matrix which provides mechanical stability and protects the bacteria from host defense. The matrix allows bacteria to adhere to each other and work as a cohesive multicellular unit to combat harsh environmental factors, distinguishing them from similar free-living bacteria [19]. These “emergent properties” developed by biofilms facilitates their survival in unsuited oral environment [7, 20].

(3) Biofilm dispersion

The final stage of biofilm development is the detachment of cells from the biofilm and dispersion into the distant sites. Biofilm dispersion processes can be categorized into three stages (1) cell detachment from the biofilm, (2) transfer of the cells to a new location, and (3) attachment of the cells to a the new location [21]. The mechanisms for biofilm dispersion are mainly characterized by active and passive mechanisms. Active

dispersion is initiated by the bacteria themselves, whereas in passive dispersion, external environmental factors such as mechanical forces from oral tissues, fluid shear forces, and abrasion play major roles [22-24]. Close relationships between species within the biofilm can result in the evolution of various other passive dispersal mechanisms including interspecific quorum-sensing signals, matrix-degrading enzymes, antimicrobial compounds [25].

Etiology of Periodontal Diseases

Based upon the observation of multiple microbial clusters, the etiology of periodontitis was established via a community ordination analysis using DNA probes [26]. From this analysis, it was observed that the microbiome composition at healthy and diseased periodontal sites changed significantly, and that certain microbes were found together repeatedly at diseased and healthy sites. Based on these observations, the microbiome was classified in five categories of red, orange, yellow, green, and purple [26]. Among these, the “red complex”, which includes *Porphyromonas gingivalis*, *Treponema denticola* and *Tannerella forsythia* appears late in the biofilm development, and was suggested to be strongly associated with adult periodontal disease progression [26-28]. However, in addition to red complex pathogens, metatranscriptome analysis of biofilms from active periodontal disease sites found that other organisms such as *Pseudomonas fluorescens* and different streptococci are also involved in transcribing virulence factors [29]. These findings suggested the role of the entire community, rather than a few pathogenic bacteria, in causing disease.

A recent understanding of disease etiology has favored the polymicrobial synergy and dysbiosis model proposed by Hajishengallis and Lamont [30]. This model suggests that dysbiosis or imbalance in the host ecosystem further leads to periodontal disease progression [30]. According to this model, *P. gingivalis* Gram-negative, anaerobic, rod-shaped bacteria plays a key role in inducing dysbiosis by modulating the innate host responses and elevating the virulence of the microbiome through interspecies signaling [30, 31]. Specifically, *P. gingivalis* is believed to alter host immune response by suppressing IL-8 and Th1 chemokines, which can result in the delayed accumulation of neutrophils, leading to uncontrolled colonization and growth of pathogenic microbiome in the oral cavity. This elevated pathogenic microbiome load (e.g., induced by *P. gingivalis*) can lead to interference in host homeostasis and tissue destruction through robust inflammation

[30], promoting the growth of subgingival asaccharolytic bacteria. These changes can induce an overgrowth of bacteria that survive well under inflammatory conditions, shifting the microbial community from a healthy to a disease causing state, further upregulating genes associated with proteolysis and inflammation [29].

These observations are further supported by an *in vivo* study performed by Hajishengallis [32]. He found that infection of wild type mice with *P. gingivalis* induces inflammation and alveolar bone resorption, both of which are characteristic of human periodontal disease. However, no such signs were found when germ free mice were infected with *P. gingivalis*, which indicates that even low abundance of *P. gingivalis* in the murine oral cavity can result in a significant increase in total biofilm biomass and population shifts in the microbial community – ultimately causing characteristic symptoms of periodontitis. Hence, in murine models, *P. gingivalis* has been considered as a key pathogen that plays a critical role in destabilizing host homeostasis and promoting a dysbiotic environment that contributes to periodontal diseases; however, it is unclear if similar events occur in humans.

P. gingivalis is widely used in the microbiological research due to its easy culture procedures and ability to alter genetic appearance [30]. *P. gingivalis* demonstrate a wide array of virulence factors that plays important role in causing tissue destruction by themselves [33]. Virulence factors such as capsule, lipopolysaccharide, fimbriae are integral parts of bacterium that is expressed at different stages of its life cycle. These determinants are capable of damaging host in different ways causing inflammation and tissue destruction [34]. In oral cavity, *P. gingivalis* can efficiently modify the host immune response and create an environment favorable to its continued persistence [35]. *P. gingivalis* alters the cytokine response of host which facilitates its own growth and accumulation of other pathogens because of suitable environment created by *P. gingivalis*. Furthermore, pro-inflammatory cytokines such as IL-1 β , IL-6 and TNF- α facilitates osteoclasts function through activation of nuclear factor kappa-B ligand [36]. Altered expression of these cytokines induces the loss of attachment and bone resorption critical for periodontal disease. The tissue destruction caused by *P. gingivalis* is majorly attributed to enhanced host immune response and increased production of these cytokines [37].

Significance of Adhesion and Invasion of *P. gingivalis* in Disease Initiation

Adhesion of *P. gingivalis* to oral tissue such as epithelial cells and the tooth surface is the first crucial step towards its colonization in the oral cavity. Extracellular structures such as fimbriae, lipopolysaccharides, internalins, and capsules play important roles (**Figure 1A**). Among these, proteinaceous structures called fimbriae are the major components involved in *P. gingivalis* adhesion to various oral structures. *P. gingivalis* is found to have two types of fimbriae: long fimbriae composed primarily of the FimA protein and short fimbriae comprised mainly of the Mfa1 polypeptide (**Figure 1B**) [38]. The long fimbriae are associated with bacterial auto-aggregation and coaggregation with *Actinomyces viscosus*, *Treponema denticola*, *Streptococcus gordonii*, and *Streptococcus oralis* [39-44]. In the absence of FimA in bacteria showed reduced adhesion of bacterial cells to gingival fibroblasts and epithelial cells [45, 46]. Additionally, the long fimbriae were found to be involved in *P. gingivalis* invasion of gingival epithelial cells. The short fimbriae are mainly associated with co-aggregation of *P. gingivalis* with *S. gordonii* [47]. In addition, recent studies highlight the importance of extracellular arginine, LPS, internalins, and the capsule of *P. gingivalis* adhesion to oral surfaces [48-54].

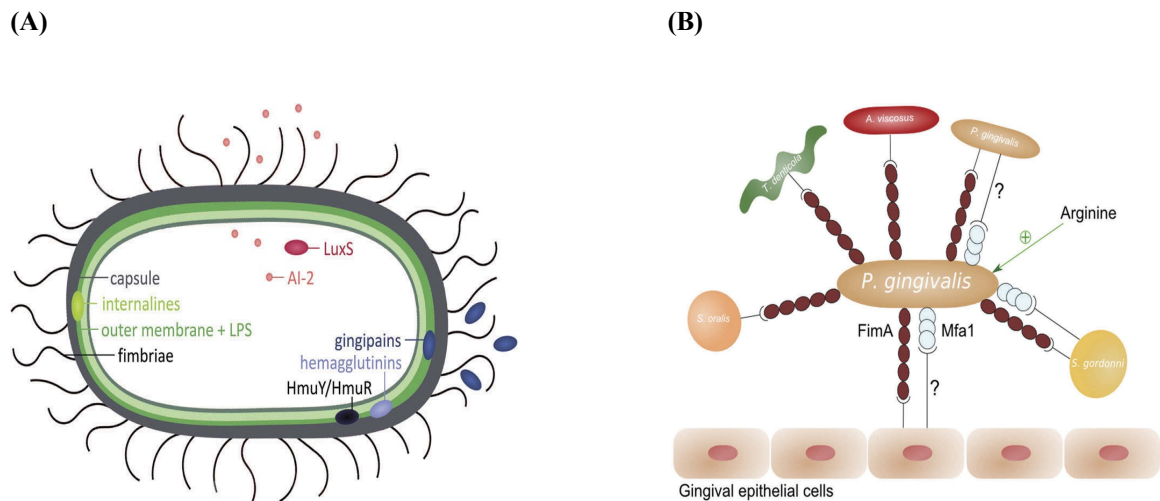


Figure 1: A. *P. gingivalis* determinants (Fimbriae, LPS, internalins, and capsule) involved in adhesion to oral structures. B. Schematics showing *P. gingivalis* fimbriae FimA and Mfa1 interactions with epithelial cells and other bacteria [55].

P. gingivalis Invasion of Gingival Epithelial Cells

Adhesion of *P. gingivalis* through these mechanisms helps to facilitate its colonization in the oral cavity and initiates bacterial invasion into gingival epithelial cells (GEC) (**Figure 2A**). Similar to many other bacterial genera such as *Salmonella*, *Shigella*, *Escherichia*, *Yersinia*, *Haemophilus*, *Listeria*, *Brucella*, *Campylobacter*, and *Actinobacillus spp.*, one of the major virulence factor of *P. gingivalis* is internalization of host cells [56-58]. Adhesion of *P. gingivalis* to the host cell surface facilitates a series of changes that lead to bacterial invasion of the cytoplasm, which protects bacteria from the host immune system and provides a suitable environment for bacterial proliferation inside the host cell [59]. Subsequently, invaded bacteria increase in number within the nutritionally rich cytoplasm of the cells and begin tissue destruction (**Figure 2B**). With the help of electron microscopy, Sandros and Lamont have observed invasion of *P. gingivalis* in multilayered human pocket epithelial cells in culture [60-62]. In general, bacterial attachment induces a series of changes that initiate structural and biochemical alterations that facilitate bacterial invasion of the cytoplasm. The interaction between bacteria and epithelial cells results in eukaryotic signaling pathways that direct phagocytosis of bacteria [63]. The host cell signaling events can induce intracellular Ca^{2+} fluxes, protein phosphorylation, and protein synthesis which may lead to reorganization of the host cell cytoskeleton to adapt the membrane invaginations that allow bacteria to enter the cell [63].

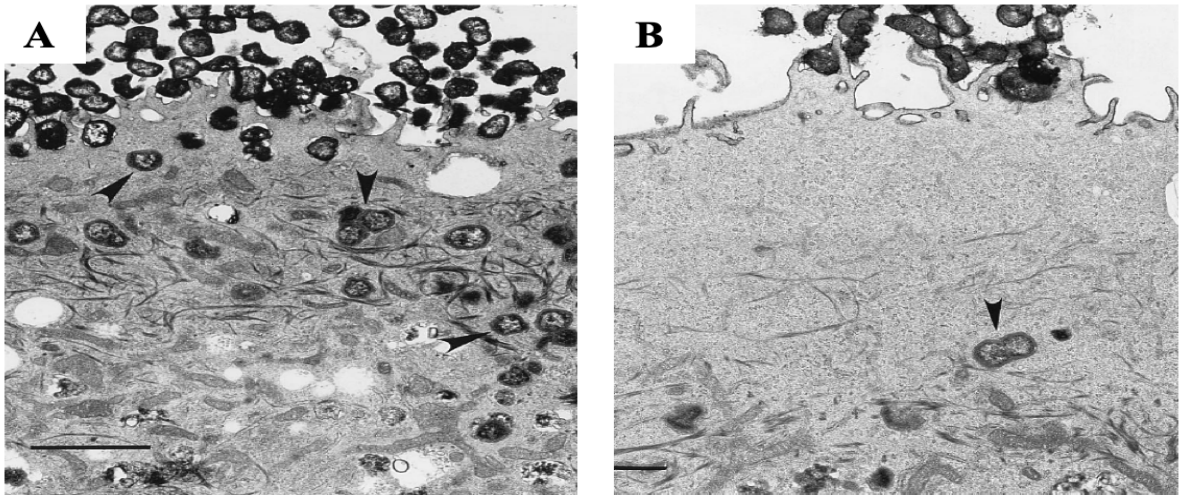


Figure 2: **A.** Image showing adhesion of *P. gingivalis* to Gingival Epithelial Cells (GECs). **B.** *P. gingivalis* invasion and proliferation inside cytoplasm. Arrows indicate invasion of bacteria inside GEC cytoplasm [60]

Treatment of Periodontitis

Treatment approaches of *P. gingivalis*-mediated periodontitis focus primarily on eradicating pathogen adhesion by mechanical debridement procedures such as scaling and root planing following the use of antiseptics or antibiotics [64-69]. The antiseptic, chlorhexidine, has been used for its broad-spectrum antimicrobial activity in the form of chips, gels, mouthwash, and films. Despite its widespread use, some of the limitations resulting from its use include tooth discoloration, taste alteration, supragingival calculus formation, and rarely, parotid swelling and oral mucosal erosion. In parallel, several types of antibiotics have been locally and systemically administered to limit *P. gingivalis*-mediated disease, including tetracyclines (tetracycline hydrochloride, minocycline, doxycycline), macrolides (erythromycin), lincosamides (clindamycin), β -lactams (ampicillin, amoxicillin), and nitroimidazoles (metronidazole) [67-69]. Systemically delivered antibiotics effectively penetrate deep periodontal pockets via serum in areas that are difficult-to-access by instruments [70]. However, there are many concerns regarding the efficacy of antimicrobial treatments. First, biofilm-residing *P. gingivalis* has been shown to be 500 times less susceptible to antimicrobial treatment compared to planktonic *P. gingivalis* [71]. Second, subgingival microflora develop antibiotic-resistance. A study indicated that 25.5%, 23.5%, and 21.6% of the *P. gingivalis* strains sequestered from periodontitis patients are resistant to amoxicillin, clindamycin, and metronidazole, respectively [72]. Additionally, pathogens such as *P. gingivalis* develop different mechanisms to evade host immune surveillance by residing within gingival epithelial cells, making periodontitis treatment even more challenging. Studies have found *P. gingivalis* within the layers of infected epithelial and connective tissue can recolonize tissues after antibiotic treatment and cause refractory disease. These limitations have prompted the need to develop novel agents to treat *P. gingivalis* mediated infections.

New Approaches to Limit *P. gingivalis* Colonization

Quorum sensing inhibitors

Bacteria in biofilms communicate with each other by producing signaling molecules termed autoinducers. Production of autoinducers is directly proportional to the density of bacteria. When bacteria reach a certain density, they initiate gene expression with the help of an intracellular signaling mechanism called quorum sensing. With the help of quorum sensing, bacteria modulate their activity and facilitate their survival in

biofilm as a community. Quorum sensing is an important mechanism to target because it induces expression of virulence factors [73]. Quorum sensing inhibitors interrupt this mechanism and present a promising treatment approach for biofilm-induced diseases. Furthermore, these inhibitors are less likely to produce bacterial resistance because they do not affect bacterial growth [74, 75]. Many of these agents are not toxic to human gingival fibroblasts and monocytic cells. Quorum sensing inhibitors such as (5Z)-4-bromo-5-(bromomethylene)-2(5H)-furanone (2 mM) and D-ribose (50 mM) have shown reduction in biofilms produced by monospecies *P. gingivalis* and dual-species *F. nucleatum* and *P. gingivalis* [42]. These inhibitors were found active in *in vivo* studies and showed decreased bone loss in a murine model of periodontitis [75-77]. In addition to these inhibitors, recent studies have evaluated a few biologics that can effectively reduce pathogenic bacterial colonization. Among them, probiotics seem to be the most promising agents to limit oral pathogens.

Probiotics: A Potential Approach to Combat Periodontitis

Elie Metchnikoff, Nobel Prize winner in Physiology and Medicine - 1908, was the first to establish the theory that the Bulgarian population had a longer lifespan due to the consumption of fermented products containing lactic acid-producing bacteria that enriched their gastrointestinal health [78]. In 1965, Lilley and Stillwell initially proposed the term “probiotic,” as opposed to “antibiotic” to define these lactic acid-producing bacteria. Etymologically, the term emerges from an amalgamation of the Latin preposition pro (“for”) and the Greek noun bios, (“life”). In 1994, the World Health Organization regarded probiotics to be the second-most important immune defense system when traditionally prescribed antibiotics were found to promote antibiotic-resistance. The WHO defined probiotics as live bacteria which, when administered in adequate amounts, confer health benefit to the host [79]. The first probiotic species, *Lactobacillus acidophilus*, was introduced in research by Hull et al. in 1984 [80]; followed by *Bifidobacterium bifidum* in Holcomb et al. in 1991 [80].

Conventionally, probiotics were associated with gut health, and their use was mainly focused on the prevention or treatment of gastrointestinal infections. However, during the last decade, the understanding of probiotic health effects have facilitated their utilization to treat a broader range of diseases such as infectious

diarrhea, skin and vaginal infection, *H. pylori* infection, and respiratory infections [80-82]. These discoveries paved the way for a new concept of probiotics in medicine and dentistry [83-85].

Emerging studies on probiotics have proposed numerous mechanisms of action (Figure 3) that include the following [79, 86]:

- 1. Probiotics bind efficiently to host surface sites resulting in inhibition of pathogen adhesion and colonization**

To date there is scarcity of *in vitro* studies that proves the exact mechanism behind probiotic effectiveness to decrease bacterial colonization. Current literature suggests that probiotics compete with pathogenic bacteria for host cell adhesion sites which results in decreased adhesion of pathogenic bacteria to the host surface [86]. This decrease in adhesion and increase in bacterial clearance results in reduced colonization of pathogens on the host surface. Higher binding efficacy of probiotics compared to pathogens is considered to be a potential reason behind this phenomenon [86, 87].

A few clinical studies performed on chronic periodontitis patients indicated decreased pathogen colonization after application of probiotics in different forms. *Lactobacillus casei Shirota* cell suspension, when incorporated in a collagenous periodontal dressing for chronic periodontitis, resulted in a decrease in the number of aggressive microbial species such as *Bacteroids*, *Actinomyces* and *Str. Intermedius*, as well as *Candida albicans* from periodontal pockets. It also extended the remission period for periodontitis up to 10 to 12 months [87]. Another study performed to evaluate *B. subtilis* effectiveness on oral health reported that *B. subtilis* applied in the form of mouthwash for 30 days significantly reduced BANA score indicative of decreased number of red complex pathogens [88]. In addition to reducing pathogenic bacterial adhesion, probiotics also possess beneficial properties suitable to treat bacterial-induced oral diseases, such as those discussed below.

2. Probiotics stimulate and modulate of the host immune system

Probiotics have been found to be effective in reducing pathogen-induced inflammation by modifying the host immune system. Probiotics have demonstrated the ability to decrease primary cytokines such as TNF and to increase secondary cytokines such as IL-6 and IL-8 in the oral cavity. They also enhance host immune response by increasing IgA and defensin and decreasing matrix metalloproteinases (MMPs). These modifications help to resolve inflammation and decrease tissue destruction [89, 90].

Shimauchi et al. stated that the regular intake of tablets (three times daily for eight weeks) containing freeze-dried *L. salivarius* resulted in lactoferrin values in gingival crevicular fluid corresponding to values in the healthy state. Lactoferrin is one of the immune components that has antimicrobial properties and normalization of its levels is indicative of the beneficial role of *L. salivarius* on pathogen-induced inflammation. Furthermore, in this study, a high-risk group of current smokers (test group) showed greater improvement of plaque index and pocket depth compared to a placebo control group. The study concluded that a probiotic intervention may be a useful tool for the treatment of inflammation and the clinical symptoms of periodontitis [90].

A more in-depth study of the molecular mechanisms underlying the beneficial effects of probiotics by Riccia and colleagues further provides insight regarding their anti-inflammatory properties of probiotics. A significant reduction in salivary levels of prostaglandin E2 (PGE2) and matrix metalloproteinases was observed after application of *L. brevis*-containing lozenges to patients with severe periodontitis cases. The authors suggested that the anti-inflammatory effects of *L. brevis* could be attributed to its ability to prevent nitric oxide production and, subsequently, the release of PGE2 and the deactivation of MMPs. However, possibilities also exist that *L. brevis* may also work as antagonist, leading to a reduction in the quantity of plaque and an improvement in the gingival index [90]. Drinking milk containing *L. casei* for 8 weeks decreased PMN elastase and MMP-3 activities in gingival crevicular fluid, and reduced gingival inflammation as measured by myeloperoxidase (MPO) activity [91].

3. Probiotics produce an environment unsuitable for pathogens

Studies also suggest that probiotics compete with disease-causing bacteria for growth factors and nutrients, resulting in the inhibition of pathogenic bacterial growth and a decrease in disease progression [86, 87]. Furthermore, many probiotics can modify the surrounding environment by regulating the pH and/or the oxidation–reduction potential, which may compromise the ability of pathogens to become established [82]. Probiotics induce antimicrobial activity by secreting products called bacteriocins, organic acids (lactic, acetic and butyric acid), and H₂O₂, which can act as antagonistics to pathogenic bacteria [92-94]. *L. acidophilus* has been shown to produce two compounds, bacteriocin lactacin B and acidolin. These compounds were found to inhibit *Lactobacilli* and enteropathogenic organisms respectively [93, 94]. Silva et al. also demonstrated an inhibitory substance produced by *Lactobacillus* GG with similar broad-spectrum activity [94]. Ishikawa et al. observed reduced *P. gingivalis*, *P. intermedia*, and *P. nigrescens* salivary counts by one-twentieth of the initial value after 4 weeks daily ingestion of *L. salivarius*-containing tablets. This inhibitory activity against periodontal pathogens was primarily related to *L. salivarius* produced acid [95].

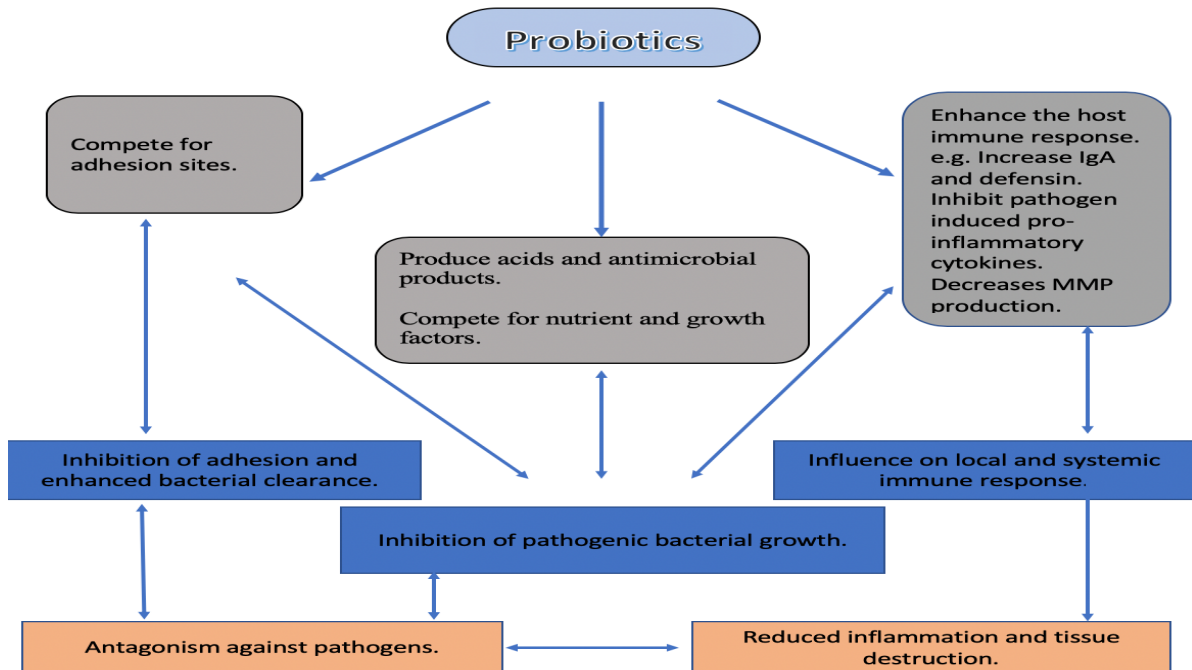


Figure 3: Schematic representation of potential mechanism of probiotics to confer health benefits to host [81]

Commonly Prevalent and Studied Oral Probiotics

Clinical studies with periodontitis patients have indicated that probiotics are capable of improving the symptoms of periodontal diseases such as bleeding on probing, inflammation, and pocket depth. Thus, probiotics may be considered as a potential therapeutic approach to combat periodontal pathogens and treat periodontal disease.

Lactobacillus spp.	acidophilus plantarum rhamnosus paracasei fermentum reuteri johnsonii brevis casei lactis delbrueckii gasseri
Bifidobacterium spp.	Breve infantis longum bifidum thermophilum adolescentis animalis lactis
Bacillus spp.	coagulans
Streptococcus spp.	thermophilus
Enterococcus spp.	faecium
Saccharomyces spp.	cerevisiae

Figure 4: Different bacterial genera classified under probiotics [96].

The most widely used oral probiotics are from the genera *Lactobacillus* and *Bifidobacterium* (**Figure 4**) [97]. These genera are observed as a part of the normal human microbiota. In the oral cavity, lactobacilli usually comprise less than 1% of the total cultivable microbiota. Species commonly isolated from saliva samples include *L. paracasei*, *L. plantarum*, *L. rhamnosus*, and *L. salivarius* [98-101]. Culture-based studies propose that bifidobacteria are among the first anaerobes to colonize the oral cavity [102]. Both lactobacilli and bifidobacteria can be found in breast milk, suggesting early exposure of the oral cavity to these bacteria [102,

103]. The most commonly isolated species from oral samples include *B. bifidum*, *B. dentium*, and *B. longum* [104-106].

Since the early writing of Metchnikoff, lactobacilli, bifidobacteria, and even more fermented food products have been regarded as safe and considered beneficial for health benefits [106]. Studies suggest that there are differences in the species composition of *Lactobacillus* and *Bifidobacterium* microbiota between periodontitis patients and healthy persons [107-109]. Various studies have conveyed the capacity of lactobacilli to inhibit the growth of periodontal pathogens, including *P. gingivalis*, *Prevotella intermedia* and *A. actinomycetemcomitans* [108]. These observations suggest that colonization of lactobacilli in the oral cavity could play an important role in the oral ecological balance. [108].

In initial studies with *L. acidophilus*, where patients with various periodontal diseases such as gingivitis, periodontitis, and pregnancy gingivitis were treated locally with a culture supernatant of *L. acidophilus*, significant recovery resulted for almost every patient [109]. Another commonly tested probiotic strain is *L. reuteri*, which is a heterofermentative bacteria that can synthesize reuterin, a small compound with antimicrobial activity [110]. After the use of *L. reuteri* in periodontitis or peri-implantitis patients, a decrease in bleeding on probing, pocket depth and gingival and plaque index was found [111-113]. Many *in vitro* and *in vivo* studies also showed that *L. reuteri* inhibits the growth of *P. gingivalis* [113-115]. Another study on *L. reuteri* and *L. brevis* has shown improved gingival health characterized by decreasing gum bleeding [114-116]. The use of chewing gum containing *L. reuteri* and *L. brevis* decreased pro-inflammatory cytokines levels and MMP (collagenase) as well as inflammatory markers in saliva, respectively [117, 118]. In another study, 14 days intake of *L. reuteri* in the form of chewing gum led to probiotic colonization in the oral cavity, resulting in a reduction of plaque in patients with moderate to severe gingivitis [118].

Guided Periodontal Pocket Recolonization

The theory of replacing the pathogenic bacteria in the periodontal pocket with beneficial bacteria is called *guided periodontal pocket recolonization*. The precise distribution of bacteria that colonizes the periodontal

pocket at any given time can be modified with the help of replacement therapy which is also known as 'probiotic therapy.' One of the pioneering studies in guided pocket recolonization showed that when a bacterial mixture containing *S. sangius*, *S. mitis* and *S. salivarius* was subgingivally applied in beagles after scaling and root planing, the recolonization of canine *P. gingivalis* and *P. intermedia* was suppressed [119]. Similarly, a delay in pathogen recolonization, a reduction in inflammation, and an improvement in bone level and density were observed when this same mixture of *S. sangius*, *S. mitis* and *S. salivarius* was subgingivally applied in a canine model [120]. These improved treatment and bone density outcomes suggest that subgingival application of probiotics may be helpful in maintaining host-bacterial symbiosis.

While these studies have widely evaluated probiotic strains in treating periodontal diseases, their actual mechanism has not been studied *in vitro*. A firm understanding of the cellular and molecular mechanisms surrounding probiotic activity will help to justify its application in treating periodontal diseases. The emergence of antibiotic resistance and the lack of natural treatment approaches highlight the need to develop approaches that utilize probiotics in periodontal treatment to complement traditional periodontitis therapy [120].

Current Probiotic Delivery Approaches and Limitations

Probiotics are widely available in the market in different dosage forms such as mouthwash, tablets, capsules, and gums. These commercially available products incorporate different probiotic genera in various dosage forms that comprise 1-3 billion CFU/serving. However, none of these products have been approved by the FDA for the treatment of oral diseases. Furthermore, even though probiotics possess beneficial properties, challenges with currently available delivery vehicles again highlight the need to develop dosage forms that are more suitable for oral treatment purposes. Current challenges of oral probiotic utilization, including the transient application of probiotics, retaining a therapeutic dose under the influence of salivary flow, and difficulties in accessing disease sites provides opportunities to improve the delivery of probiotics (and other active agents) to treat periodontitis. To date, there is a dearth of orally-administered sustained-release dosage forms that provide prolonged delivery (> 1 wk.) within the oral cavity. Furthermore, few dosage forms have

the ability to incorporate and maintain the viability of probiotics during oral application. Therefore, the development of new delivery vehicles that provide localized sustained-release within the oral cavity would help to address these limitations.

Novel Delivery Approach

In the last few years 3D-printing has been explored for medical and dental applications. Recent advances in both techniques and materials for 3D-printing have demonstrated the feasibility of this technology for regenerative medicine, tissue engineering, and biomedical research (**Figure 5**). 3D-bioprinting can be defined as a process of combining cells with suitable polymers to create a cell-laden 3D-printed construct for tissue engineering, drug screening, or *in vitro* disease models [121]. In 3D-bioprinting, a polymer solution containing cells, called a bioink, is used to fabricate a complex three-dimensional scaffold-like geometry (**Figure 5**). For many eukaryotic cell applications, bioinks have served as an extracellular matrix to facilitate eukaryotic cell adhesion, proliferation, and differentiation [122]. However, 3D-bioprinting has been less explored for the delivery of prokaryotic cells, in particular for therapeutic applications. With the availability of a wide variety of materials and different printing techniques, 3D-bioprinting provides a suitable platform to utilize prokaryotic cells for therapeutic purposes. Selection of a desirable bioink plays a crucial role to facilitate cell-based applications and is mainly based on the type of incorporated cells and characteristics of the polymer (**Figure 6**). Previous studies have applied 3D-printing to generate human bone, skin grafts, myocardium, corneal tissue, trachea, intestinal tissue using different materials, bioactive agents, and most importantly prokaryotic bacterial cells. [123-128].

Advantages of 3D-Bioprinting

- **Shape customization**

3D-bioprinting provides a number of advantages relative to other methodologies of formulating three dimensional scaffolds. The ability to rapidly customize shapes, with high printing resolution, is the biggest advantage of 3D-printing. Precise shapes and geometries of different scaffolds can be created for custom applications with the help of commercially available software.

- **Freedom of creating complex architecture**

In addition to finely tailoring shapes and geometries, 3D-printing has the potential to create complex, multilayered structures by employing various printing techniques and combining multiple materials of suitable properties. Previous studies have created skin grafts, myocardium, corneal tissue, trachea, and intestinal tissue by incorporating different 3D-printing techniques [127-131].

- **Wide variety of material of choice**

3D-bioprinting utilizes a wide variety of natural and synthetic printable materials that can support the viability and growth of different kinds of eukaryotic cells, growth factors, stem cells, etc. Properties of bioink can also be modified by combining two or more different materials [132].

- **Less time consuming and technique sensitive**

Relative to the fabrication approaches involved in other dosage forms (e.g., molded structures, nanoparticles, and electrospun fibers), 3D-printing is a less time consuming process. 3D-printing takes anywhere from minutes to an hour to print a scaffold, depending on the desired size and shape. Other alternatives such as molded scaffold synthesis can take as long as 10 to 12 hr to fabricate, whereas 3D-printing requires minimal effort to manufacture the scaffolds as compared to more time-intensive fabrication techniques.

- **High throughput**

High throughput is possible with 3D-printing because of the comparatively fast nature of the procedure, minimal opportunities for user error, low equipment maintenance, and low manufacturing cost of scaffolds. These potential advantages make 3D-printing a promising method with which to fabricate novel dosage forms for probiotic administration in the oral cavity.

Stepwise Procedure for Bioprinting

The 3D-printing procedure can be divided into the following stages.

- **Pre-printing:** The pre-printing stage includes the growth and culture of cells, selection of suitable printing material based on the type of cells, bioink preparation, and development of a program to operate the printer and create customized shapes.
- **Printing:** During the printing stage, printing parameters including temperature and pressure are adjusted as the bioink is printed.
- **Post-printing:** The post-printing stage consists of mechanical and chemical alteration of the scaffolds via crosslinking.

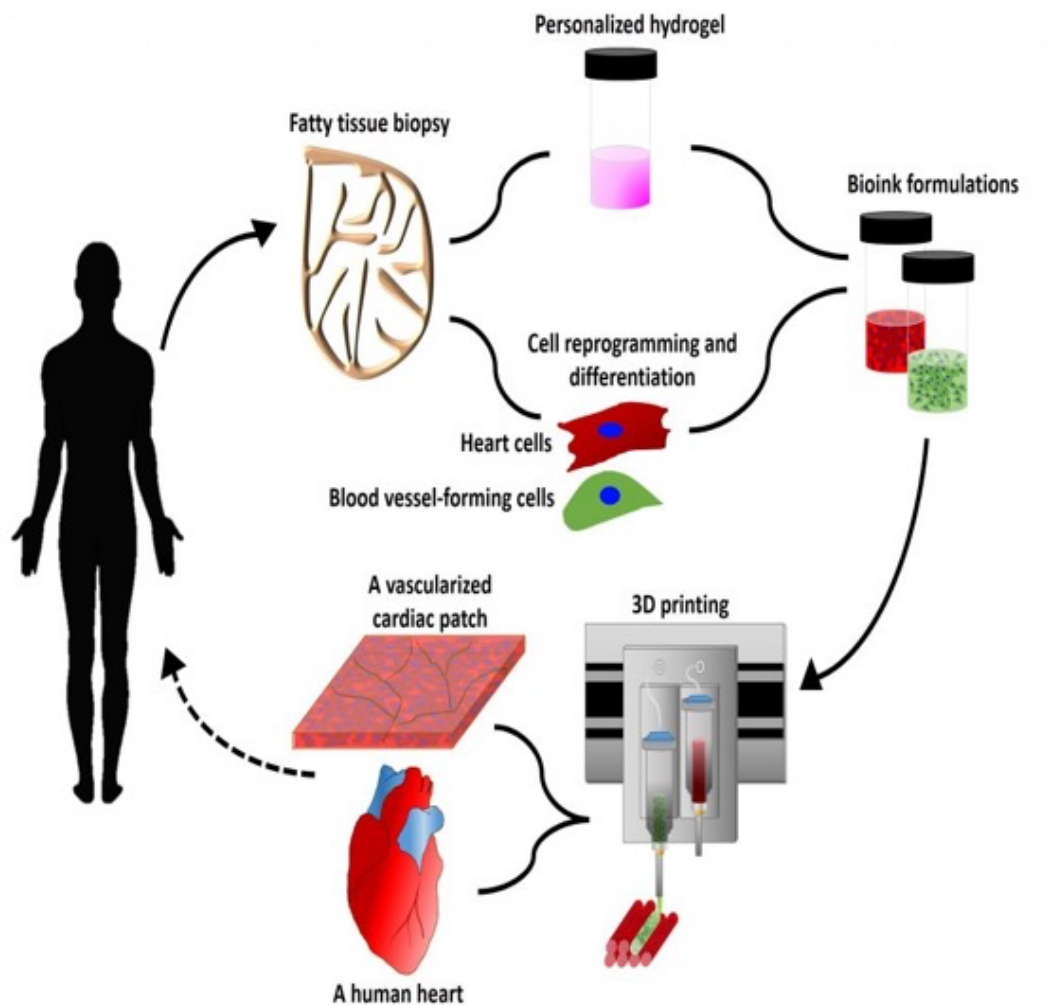


Figure 5: Schematic representation of stepwise procedure for 3D-bioprinting.

Image adapted from: <https://www.zmescience.com/research/inventions/3d-printing-heart-15042019> [133].

Classification of Bioprinting Materials

A schematic of different bioink categories is provided in Figure 6 and their characteristics are described here.

- **Matrix bioinks**

Matrix bioinks protect cells from external environmental factors such as shear stresses during the printing process. Matrix bioinks closely mimic the extracellular matrix and offer quick, nontoxic gelation to achieve optimal print resolution. These bioinks range from media suspended cell slurries to cell-laden hydrogels such as polyethylene glycol (PEG), gelatin or alginate [134-136]

- **Sacrificial bioinks**

Sacrificial bioinks are temporary inks that can be washed away after printing. They are mainly used to develop a vascular network in a complex geometry. Sacrificial polymers offer high print fidelity, cytocompatibility and ease of removal after printing [137, 138].

- **Support bioinks**

Support bioinks offer more lasting support than sacrificial bioinks. Support biomaterials enhance mechanical properties when used with matrix bioinks. These materials are most useful when developing tissues that require higher mechanical strength, such as bone or cartilage. Support biomaterials include thermoplastics such as polycaprolactone, poly(lactic-co-glycolic acid) or polylactic acid [139-142].

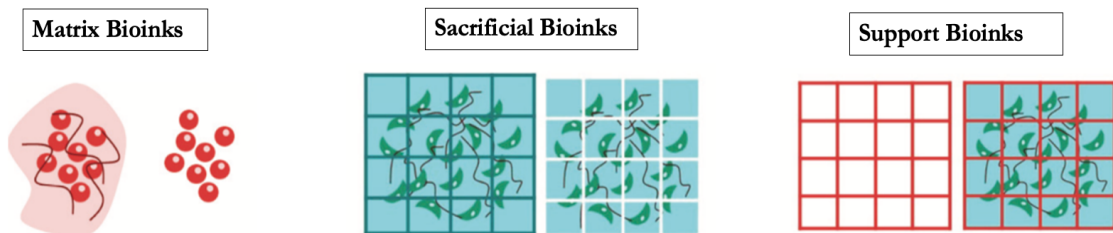


Figure 6: Illustration of different categories of bioinks [134].

Alginate-Gelatin Bioink

Among currently available biopolymers, gelatin and alginate are attractive for bioprinting applications because of their ability to sustain cell viability and provide mechanical stability to printed scaffolds. Alginate is a natural biopolymer obtained from brown algae. It is a negatively charged polysaccharide, which is bioinert and induces a negligible inflammatory response *in vivo*. Alginate is made up of two repeating monomer units (1–4)- β -D- mannuronic acid and α -L-guluronic acid. α -L-guluronic acid helps the gel to solidify, whereas the (1–4)- β -D- mannuronic acid and its combination with α -L-guluronic acid assist in increasing the flexibility of the material [143-145]. Alginate can be easily modified by altering the polymer density and crosslinking techniques [146-148]. Alginate biopolymers entrap water and other molecules by using capillary forces and can allow it to diffuse from inside out. This characteristic is ideal for 3D-bioprinting to achieve sustained release of biologics and other active agents from the bioprinted scaffolds [149, 150]. However, alginate does not interact with cells and therefore, cannot provide cell adhesion and differentiation. Because of these limitations it is mostly used with gelatin [151]. Gelatin is a denatured form of collagen capable of reversible thermal gelation. Gelatin together with alginate increases the viscosity of alginate and improves print fidelity. Gelatin also has abundant integrin-binding motifs, such as fibronectin, vimentin, and vitronectin, which are usually helpful in eukaryotic cell migration, adhesion, and tissue repair [152].

Currently Available Techniques for 3D-Bioprinting

To date, there are several different bioprinting techniques to accommodate the properties of various printing materials (**Figure 7**). Among these, extrusion-based, fused deposition modeling, inkjet, stereolithography, and laser-assisted techniques are the most widely used. Selection of the technique for bioprinting is mainly dependent on the type of bioink. To illustrate, extrusion-based printing is the most common technique to use pressure to print the material [153-159]. Hence, it is most suitable to print hydrogels. Another technique, somewhat similar to the extrusion-based method, is fused deposition. This technique combines pressure and high temperature to fuse the materials. Fused deposition printing, while similar in other ways to extrusion, is best suited for thermoresponsive polymers and plastics [160, 161]. The high temperature conditions, make it

less amenable for live cell incorporation. Inkjet printing is a droplet-based method that uses a thermal or electrostatic actuator, and is therefore efficient in printing low viscosity inks [162-171]. Stereolithography and laser-assisted printing rely on laser or UV curing. These techniques are mainly used for bioinks requiring a photo-initiator [172-174] and can be detrimental to cell viability.

For our applications, we have utilized an extrusion-based bioprinting method, which enables materials to print within physiologically relevant temperature and pressure ranges, to maximize cell viability in printed scaffolds. Extrusion printing enable factors such as laser wavelength and high temperatures to be excluded from the printing process. Gelatin and alginate hydrogel bioinks can be most efficiently printed using an extrusion-based technique without compromising incorporated bacterial cell viability. In extrusion bioprinting, a bioink-containing syringe is dispensed through the nozzle by pneumatic pressure or mechanical force [153]. The pneumatic system uses compressed air to force the bioink out of a nozzle orifice. This process takes some time to build up pressure for printing according to Bernoulli's principle of fluids [154]. A mechanical dispensing system uses a screw or piston for extrusion-based printing which can be controlled robotically resulting in more spatial control over bioink extrusion. The more complex design of an extrusion-based printer relative to a pneumatic system, which makes it more prone to malfunction, is its main shortcoming. Extrusion bioprinters are capable of printing high viscosity materials including hydrogels, biocompatible copolymers, and cell spheroids. These attributes, together with low temperature and solvent-free printing capabilities, make extrusion bioprinting an advantageous method to print probiotic-containing scaffolds for oral delivery.

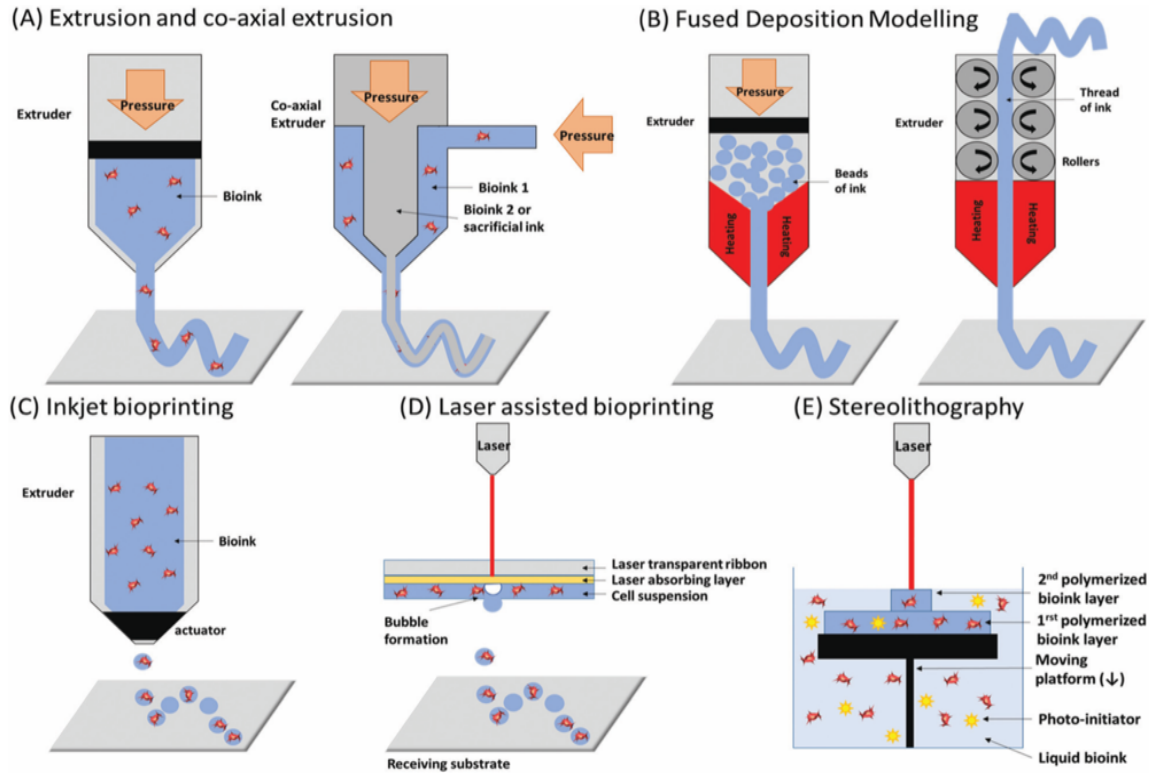


Figure 7: Schematic representation of different bioprinting techniques [163].

CHAPTER 2

HYPOTHESIS AND SPECIFIC AIMS

Antibiotics are most commonly used as adjuncts to mechanical manipulation for periodontal treatment to limit disease reoccurrence. However, antibiotic treatment has some limitations in achieving long-term efficaciousness, which is attributed to: (1) biofilm-mediated protection, (2) antibiotic resistance, and (3) internalization of *P. gingivalis* into GECs and recolonization of the oral cavity after treatment. The long-term aim of this project was to decrease antibiotic use by developing a novel approach to limit *P. gingivalis* colonization. Toward this goal, we aimed to assess the ability of selected probiotics to reduce *P. gingivalis* adhesion and invasion into TIGKs and to promote and increase TIGK cell viability. We selected *Lactobacillus reuteri*, *Lactobacillus acidophilus*, and *Bifidobacterium bifidum* from among the most clinically evaluated probiotics, for additional evaluation *in vitro*. In parallel, we explored the application of 3D-bioprinting to develop an alternative approach to incorporate probiotics with high viability for localized oral delivery. Our hypothesis was that 3D-printed scaffolds prepared using gelatin alginate bioink would incorporate and sustain the release of highly viable probiotics for 7 to 14 days.

Specific Aims to achieve these goals:

Aim 1: Evaluate the ability of *Lactobacillus reuteri*, *Lactobacillus acidophilus*, and *Bifidobacterium bifidum* to prevent *P. gingivalis* adhesion to, and invasion of, TIGK cells and determine the resultant modulation of TIGK cell viability.

Aim 2: Develop and characterize 3D-printed gelatin-alginate scaffolds that maximize probiotic viability and sustain the release of probiotics for ~7 to 14 days.

CHAPTER 3

MATERIAL AND METHODS

Growth of Bacterial Strains

Porphyromonas gingivalis ATCC 33277 (*P. gingivalis*) was cultured in Trypticase soy broth medium (TSBY medium, Difco Laboratories Inc., Livonia, MI, USA) supplemented with 0.5% (w/v) yeast extract, 1 µg/ml menadione, and 5 µg/ml hemin. The growth medium was reduced for 24 hr in an anaerobic chamber (10% CO₂, 10% H₂, and 80% N₂). Twenty ml of reduced media was subsequently inoculated with 2 ml of an overnight *P. gingivalis* culture and incubated under anaerobic conditions for 48 hr at 37°C. *Lactobacillus acidophilus* ATCC 4356 (*L. acidophilus*) and *Lactobacillus reuteri* ATCC 23272 (*L. reuteri*) were cultured in de Man, Rogosa & Sharpe broth (MRS Broth) (Sigma-Aldrich, MO, USA). Briefly, 10 ml of medium was inoculated with 100 µL of previously cultured bacteria and incubated at 37°C under aerobic conditions. *Bifidobacterium bifidum* ATCC 29521 (*B. bifidum*) was cultured in a Modified Reinforced Clostridial medium (ATCC® Medium 2107). The culture medium was pre-reduced for 2 hr in an anaerobic chamber. Ten ml of pre-reduced media was sub-cultured with 1 ml of previously cultured *B. bifidum* medium. The culture medium was incubated in anaerobic conditions for 48 hr. For the procedures below, the desired concentration of bacteria was obtained by centrifuging 10 ml of bacterial medium at 3500 x g for 10 min. Centrifuged bacteria were then resuspended in 1ml PBS and the OD₆₀₀ of the bacterial solution was measured by diluting 50 µl of solution in 950 µl of PBS. The final optical density was calculated by multiplying the dilution factor (20x) with the machine reading. Desired Multiplicity of Infection (MOI) of the cell suspensions was calculated based on the final OD₆₀₀ using standard curves relating bacterial cfu and culture OD₆₅₀ for each organism.

Cell Culture

In our experiments, we utilized telomerase immortalized gingival keratinocytes (TIGKs), which are a viral protein-modified cell line derived from gingival epithelial cells found in the oral cavity [175]. They are typically used in *in vitro* experiments due to their infinite life span and reduced donor-to-donor variability. TIGKs were grown in T75 flasks and cultured using DermaLife K Calcium Free Medium (LifeFactors®) supplemented with penicillin/streptomycin (100 U/ml final concentration: St. Louis, MO), L-glutamine (6 mM), epinephrine (1 µM), recombinant human (rh) insulin (5 µg/ml), apotransferrin (5 µg/ml), rhTGF-α (0.5 ng/ml), extract PTM, hydrocortisone hemisuccinate (100 ng/ml), and calcium chloride (0.06 mM). The epithelial cells were incubated at 37°C in the presence of 5% CO₂ for one week to obtain 70% confluency.

Evaluation of binding efficacy of *P. gingivalis* to TIGKs after labeling with CS and HI

Among widely used fluorescent dyes, carboxyfluorescein succinimidyl ester (CS) stains extracellular constituents such as the cell wall and outer membrane proteins via its succinimidyl group. Hexidium iodide (HI) is a nucleic acid staining dye that selectively stains DNA. The binding efficiency of *P. gingivalis* to TIGKs, after labeling with carboxyfluorescein succinimidyl ester (CS) and hexidium iodide (HI), was evaluated to determine the most suitable dye for labeling *P. gingivalis*. CS- and HI-labeled *P. gingivalis* were applied to TIGKs (1x10⁵ cell/well) at MOIs of 100, 1000, and 5000 for 90 min. The number of CFUs of cell-bound *P. gingivalis* was determined by converting each fluorescence value to the number of CFU counts per mL with the help of a fluorescent standard curve.

Adhesion Assay

P. gingivalis adhesion to TIGK cells was evaluated after pre- or co-treatment with *L. acidophilus*, *L. reuteri*, or *B. bifidum*, administered individually and at varying concentrations to a confluent layer of TIGKs. First, TIGK cells were trypsinized and plated in 24-well plates at a density of 1x10⁵ cells per well. After 48 hr at 37°C in the presence of 5% CO₂, cells were treated with carboxyfluorescein succinimidyl ester (CS)-labeled *P. gingivalis* at a multiplicity of infection (MOI) of 2000 for the positive control group. Untreated TIGKs

were considered a negative control group for background fluorescence and a lack of *P. gingivalis* adhesion. Adhesion of the probiotic strains to TIGK cells in the absence of *P. gingivalis* was evaluated by individually labeling them with CS and administering them to TIGK cells at MOIs of 500, 1000, 2000.

After demonstrating adhesion of each fluorescently-labeled probiotic group alone, the ability of probiotics to inhibit *P. gingivalis* adhesion was evaluated. In the first experimental group, TIGKs were pre-treated with unlabeled probiotic strains at different MOIs for 15 min, and subsequently treated with fluorescently (CS)-labeled *P. gingivalis* at a MOI of 2000 (**Figure 8**, pre-treatment). In the second experimental group, CS-labeled *P. gingivalis* was applied at a MOI of 2000 and unlabeled probiotics were applied at MOIs of 500, 1000, 2000 and co-cultured with *P. gingivalis* (**Figure 8**, co-treatment). Bacteria-treated TIGKs were incubated for 90 min at 37°C in the presence of 5% CO₂ to allow for bacterial adhesion. After incubation, the supernatant was removed and TIGKs were washed three times with phosphate buffered saline (PBS) (137 mM NaCl, 2.7 mM KCl, 8 mM Na₂HPO₄, and 2 mM KH₂PO₄). Fluorescence of *P. gingivalis* adhered to TIGKs was measured using a SpectraMax analyzer at 485 (excitation) and 535 (emission) nm wavelengths. The fluorescence curves for *P. gingivalis* were prepared by serially diluting 2x10⁸ CS labeled bacterial cells per 0.5 mL and measuring the subsequent fluorescence. Adhered *P. gingivalis* bacterial colony forming unit (CFU) counts were determined by converting fluorescence to CFUs with the help of this standard fluorescence curve.

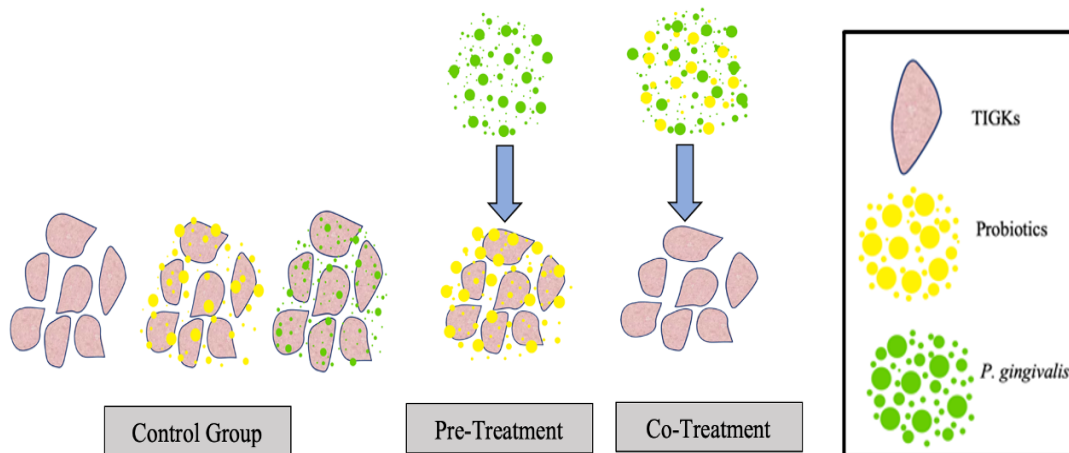


Figure 8: Schematic representing control and experimental groups of the adhesion assay. Control groups consisted of untreated TIGKs, fluorescently-labeled *P. gingivalis*-treated TIGKs, and fluorescently-labeled

probiotic-treated TIGKs. Experimental groups include pre-treatment with unlabeled probiotics followed by fluorescently-labeled *P. gingivalis* treatment or simultaneous co-treatment of TIGKs with fluorescently-labeled *P. gingivalis* and unlabeled probiotics. Carboxyfluorescein succinimidyl ester (CS) was used to label probiotics for binding efficiency experiments or *P. gingivalis* for adhesion assays as described in the Methods.

Antibiotic Protection Assay to Measure *P. gingivalis* Invasion of TIGK Cells

P. gingivalis invasion of TIGKs was quantified using an antibiotic protection assay (**Figure 9**). After measuring cell-bound fluorescence in the adhesion assay, adherent cell-bound bacteria were removed by incubating TIGK cells with 300 µg/ml gentamicin and 500 µg/ml metrinidazole for one hour at 37°C in the presence of 5% CO₂. Following incubation with antibiotics, TIGKs were treated with 500 µl of sterile DI water to lyse the cells and released *P. gingivalis* (bacteria inside TIGKs) was quantified by plating 50 µl of the suspension on blood agar plates supplemented 0.5% (w/v) yeast extract, 1 µg/ml menadione, and 5 µg/ml hemin, 0.5 µg/ml Streptomycin. Plates were incubated under anaerobic conditions for 6 days. The invasion was determined by counting CFUs [47].

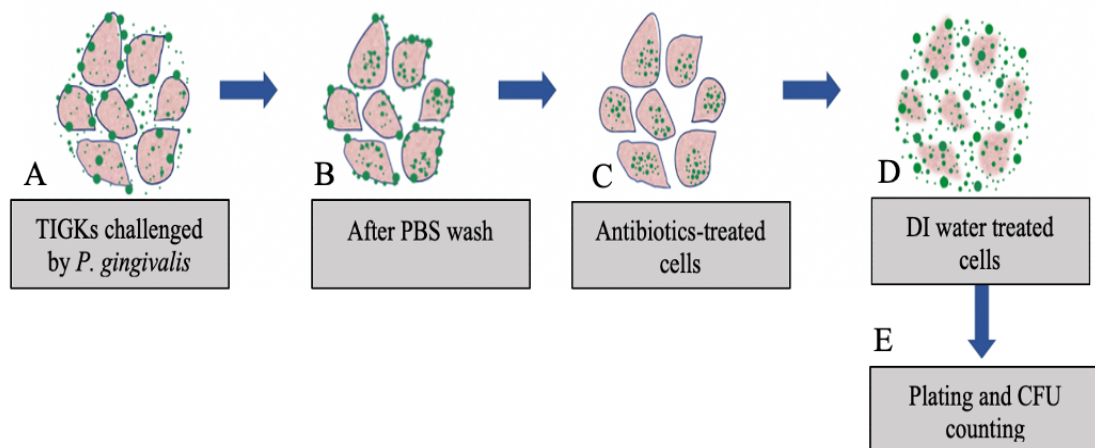


Figure 9: Overview of antibiotic protection assay. **A.** TIGKs treated by *P. gingivalis*. **B.** Removal of unbound *P. gingivalis* by PBS wash. **C.** Killing of cell bound *P. gingivalis* by antibiotics treatment of TIGK cells. **D.**

Treatment with DI water to collect internalized *P. gingivalis* by breaking the cell wall. E. Plating of supernatant and CFU counting.

Lactate Dehydrogenase Assay (LDH Assay)

TIGK viability after treatment with *P. gingivalis* was evaluated by using the CytoTox 96[®] Non-Radioactive Cytotoxicity Assay kit (Promega, WI, USA). An initial experiment was performed to determine the effect of TIGK cell density and cell lysis on LDH expression. Briefly, 2.5×10^4 , 5×10^4 , 1×10^5 , and 2×10^5 TIGK cells per well were plated for 48 hr. Untreated/unlysed TIGKs and LDH (+) provided by the manufacturer served as a negative and positive controls for LDH expression, respectively.

LDH expression from unlysed and lysed TIGKs of the same density was determined, and the cell density that resulted in maximum LDH expression between unlysed and lysed cells (5×10^4) was selected for further experiments. The effects of *P. gingivalis* administration on TIGKs was evaluated by applying MOIs of 100, 500, 1000, 2500, 5000 and assessing LDH release from the cells. TIGKs were plated at density of 5×10^4 cells per well for 48 hr before the experiment and incubated at 37°C in the presence of 5% CO₂. On the day of experiment, cells were treated with *P. gingivalis* (MOIs of 100, 500, 1000, 2500, and 5000) and incubated for 8 hr. The experiment had three groups: a negative control of untreated/unlysed TIGKs, a positive control of untreated/lysed TIGKs, and an experimental group of *P. gingivalis*-treated TIGKs. To exclude effects of bacterial acid production on experimental results, we prepared free *P. gingivalis*-only cultures to measure LDH production by *P. gingivalis* and subtracted these background levels from the experimental groups. Forty-five minutes before collecting the supernatants, the positive control group was treated with 50 µl of lysis solution (10x) provided by the manufacturer to attain maximum LDH release from the cells. After the total incubation time of 8 hr, plates were centrifuged at 250 x g for 4 min and 50 µl aliquots from each group was transferred to 96-well plates. Fifty µl of CytoTox 96[®] Reagent was then added to each well and incubated for 30 min at 37°C in the presence of 5% CO₂. The reaction was terminated by adding a stop solution of 50 µl into wells. Absorbance was measured at 490 nm and the percent cytotoxicity was calculated using the following equation where effector spontaneous = *P. gingivalis*-alone; TIGK spontaneous = TIGKs only; Lysed TIGKs = target maximum of LDH expression/release.

$$\% \text{ Cytotoxicity} = \frac{\text{Experimental} - \text{Effector Spontaneous} - \text{TIGKs Spontaneous}}{\text{Lysed TIGKs} - \text{TIGKs Spontaneous}} \times 100$$

Preparation of Bioink for 3D-Printed Scaffold

Bioink preparation without bacteria:

A 10% gelatin:2% alginate bioink was prepared by adding 500 mg of gelatin (gel strength – 225 bloom, ~50 kDa Sigma, MO, USA) and 100 mg of alginate (viscosity not provided, MP Biomedicals, LLC, OH, USA) to 5 ml of sterile MRS broth in a scintillation vial. Bioink was vortexed to prepare a homogenous mixture. This preparation was incubated at 37°C overnight to completely dissolve the polymer.

Bioink preparation with bacteria:

Probiotic-containing bioinks were prepared by adding 500 mg gelatin and 100 mg alginate to 4.5 ml of sterile MRS broth. The bioink (without probiotics) was similarly vortexed and incubated at 37°C overnight. On the day of printing, probiotics were added to the ink by centrifuging MRS broth containing 5×10^7 bacteria per mg of polymer at 3500 x g for 10 min. The probiotic pellet was resuspended in 0.5 mL of fresh MRS broth and the prepared solution was added to the bioink. The ink was vortexed and incubated at 37°C for 15 min to ensure distribution of probiotics throughout the ink.

3D-Bioprinting of Scaffold

3D scaffolds were printed with the help of an Allevi 3 bioprinter (Allevi, Inc., PA, USA) (Figure 10). STL files were created by SolidWorks software to print 13 x 1 mm scaffolds. STL files were converted into G-code by Allevi 3 software and scaffolds were printed adjusting parameters like temperature, pressure, and needle gauge size. Scaffold bioprinting conditions were set to: 37.5°C, 42 psi and a 29 gauge needle.

Scaffold Crosslinking

Immediately after printing, scaffolds were stored in the refrigerator at 4°C for 15 min. The scaffold strength and structural stability were enhanced by crosslinking alginate and gelatin with CaCl₂ (Fisher Scientific) and

genipin (Fisher Scientific), respectively. Alginate crosslinking was performed first by treating scaffolds with 5 mL 10% w/v CaCl_2 in water at 4°C for 15 min. Following alginate crosslinking, scaffolds were treated with 5 mL 0.5% w/v genipin solution in DI water for 4 hr at room temperature to crosslink gelatin in the scaffolds.

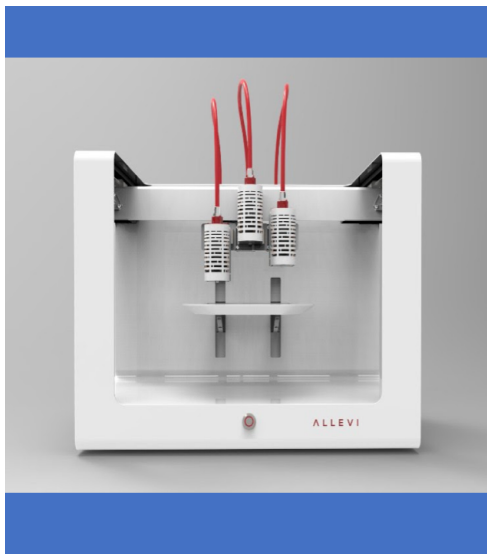


Figure 10: Allevi 3 bioprinter with three extruders.

Image adapted from: <https://3dprint.com/wp-content/uploads/2018/09/unnamed-40.jpg> [176].

Viability of Probiotics in 3D-Bioprinted Scaffolds

The working temperature and pressure of the printer during scaffold preparation affects the viability of probiotics. Therefore, it was important to determine the number of viable cells present after printing (**Figure 11**). 3D-bioprinted scaffolds were incubated at 4°C for 10 min. Uncrosslinked scaffolds were weighed and transferred into 1.5 mL eppendorf tubes. One ml of MRS broth was added into each tube and incubated at 37°C for 10 min. Once scaffolds completely dissolved into the medium, the resultant solution was serially-diluted and 5 μl of the solution was plated on agar plates. The number of CFUs/mg was calculated to determine the number of viable bacteria in the scaffold after printing. The difference between bacterial CFU/mg initially added to the bioink and CFU/mg calculated after 3D-printing provided the percent viability of the probiotics in the 3D-bioprinted scaffolds.

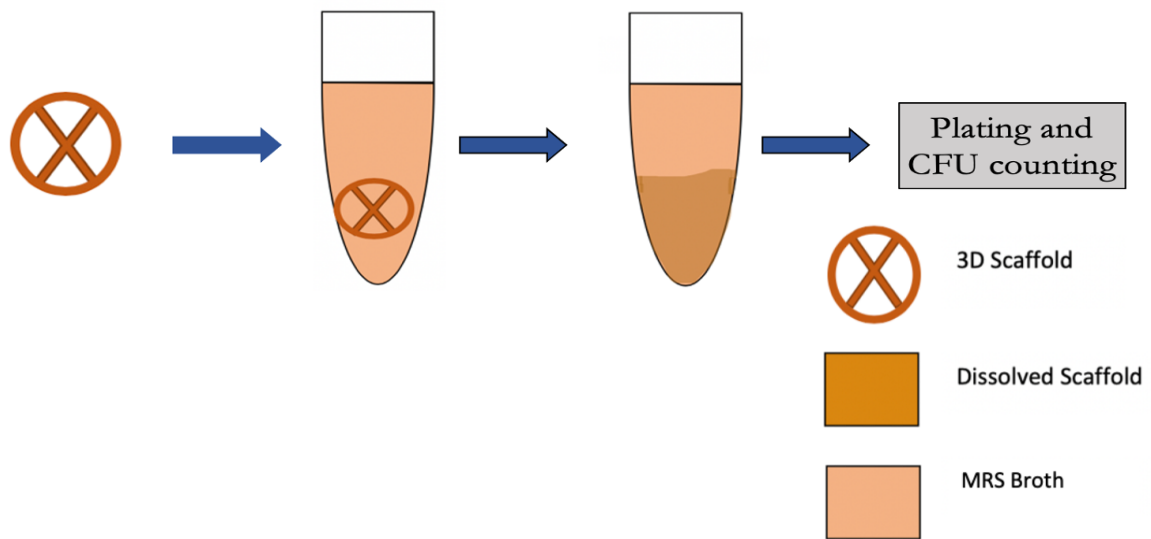


Figure 11: Overview of steps involved to determine post-print viability. Schematic shows the dissolution of the scaffold in MRS medium, plating of this solution, and CFU counting of probiotics from the dissolved scaffold.

Probiotic Release from 3D-Printed Scaffolds

Probiotic release was evaluated at different time points of 1, 2, 4, 8, 24, 48 hr, and each day up to 2 weeks to evaluate the potential of scaffolds to sustain probiotic release (**Figure 12**). The scaffold was weighed to record its initial mass and then 5 mL of the media (1 X PBS, MRS broth, or artificial saliva (Pickering laboratories, 1700-0305) was added to each eppendorf tube and incubated at 37°C between time points. To measure release, media (complete 5 ml) was removed for measurements daily and 100 µl of this eluate was serially diluted to determine CFU counts. Bacterial CFU counts were determined by plating 5 µL of each sample dilution on MRS agar plates. Plates were stored for 48 hr in anaerobic conditions at 37°C. The CFU/mg of each sample was calculated and probiotic release from the scaffold at 1, 4, 8, 24, 48, 72 hr, and each day was determined. After removing supernatant for plating, scaffolds were washed three times with 1 x PBS to remove bacteria present on the surface. The scaffolds were resuspended with fresh 5 ml of the medium of choice and incubated at 37°C until the next time point.

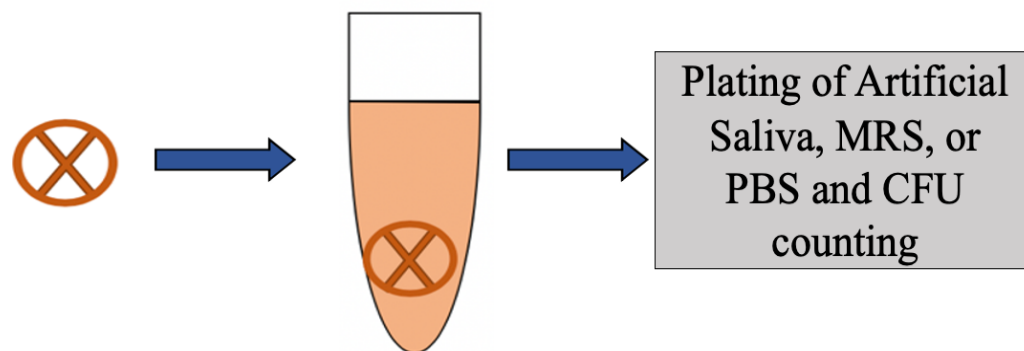


Figure 12: A brief illustration of release assay procedure. Schematic showing plating of solution and CFU counting after incorporation of scaffolds in artificial saliva, MRS, or PBS until each desired time point.

CHAPTER 4

RESULTS

Specific Aim 1:

Aim 1: Evaluate the ability of *Lactobacillus reuteri*, *Lactobacillus acidophilus*, and *Bifidobacterium bifidum* to prevent *P. gingivalis* adhesion to, and invasion of, TIGK cells and determine the resultant modulation of TIGK cell viability.

Results from the *P. gingivalis* Adhesion Assay

Evaluation of binding efficacy of *P. gingivalis* to TIGKs after labeling with CS and HI:

The binding of *P. gingivalis* to TIGKs, after labeling with carboxyfluorescein succinimidyl ester (CS) and hexidium iodide (HI), was evaluated to determine the labeling efficacy and most suitable dye with which to label *P. gingivalis*. While both CS- and HI-labeled *P. gingivalis* demonstrate a dose-dependent trend in binding to TIGK cells, a comparison of the labeling efficiency indicated that CS labels *P. gingivalis* more efficiently (**Figure 13**). Overall, higher *P. gingivalis* binding to TIGKs was observed with CS, relative to HI labeling at all concentrations. This indicates that regardless of the double ester bond in CS (which may interfere with *P. gingivalis* binding), that CS labels *P. gingivalis* more efficiently than HI, enabling *P. gingivalis* binding to be more easily detected, on TIGK cells.

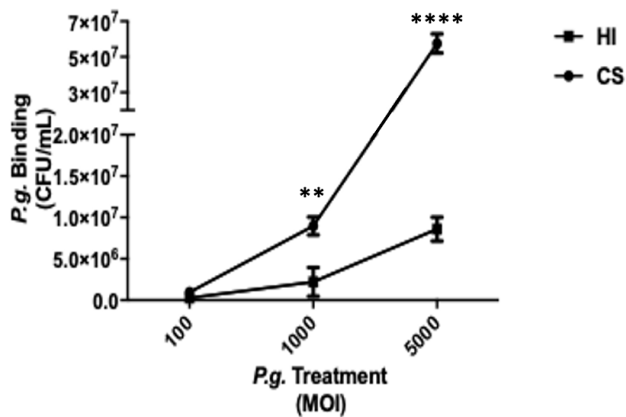


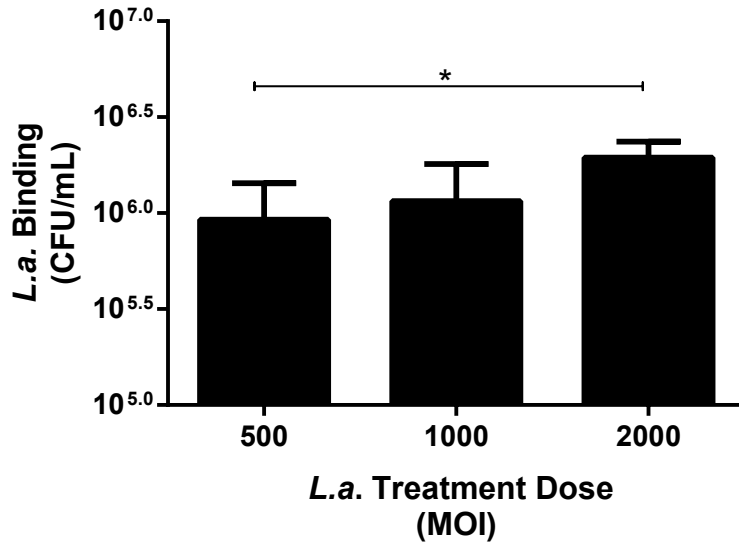
Figure 13: Carboxyfluorescein succinimidyl ester (CS)-labeled *P.g.* showed increased adhesion to TIGK cells, relative to hexidium iodide (HI)-labeled *P.g.* under different dosing conditions. zTIGK cells, plated at a density of 1×10^5 cells per well, were treated with CS- and HI-labeled *P.g.* at MOIs of 100, 1000, 5000 for 90 min. Fluorescence, indicative of *P.g.* binding, was measured (485 nm ex/535 nm em) and the number of CFU/mL were determined. Values represent the mean \pm standard deviation of CFU/mL of *P.g.* adhered to TIGK cells. A statistically significant increase in adhesion was observed when *P.g.* was labeled with CS at MOIs of 1000 and 5000 (** $P \leq 0.01$, **** $P \leq 0.0001$).

Free *L.a.* adheres to TIGK cells and reduces *P. gingivalis* adhesion to TIGK cells

TIGK cells treated with different MOIs (500, 1000, and 2000) of *L. acidophilus* in the absence of *P. gingivalis* demonstrated a dose-dependent trend in *L. acidophilus* binding; however, statistical significance was only observed between *L. acidophilus* applied at an MOI of 500 and 2000 (**Figure 14A**, * $P \leq 0.05$). Next, we evaluated the ability of free *L. acidophilus*, administered as a pre- or co-treatment at MOIs of 500, 1000, and 2000, to inhibit *P. gingivalis* binding to TIGK cells (**Figure 14B**). A dose-dependent reduction in adhesion of *P. gingivalis* (MOI 2000) was observed after pre-treatment with probiotics (** $P \leq 0.01$, *** $P \leq 0.001$). Pre-treatment with *L. acidophilus* for 15 min at MOIs of 500, 1000, and 2000 reduced adhesion by 53%, 56%, and 68%, respectively, relative to *P. gingivalis* alone.. In comparison, co-treatment of free *L. acidophilus* at MOIs of 500, 1000, 2000 with *P. gingivalis* (MOI 2000) showed a trend in reducing *P. gingivalis* binding. Specifically, administration of *L. acidophilus* at an MOI of 2000 significantly decreased

P. gingivalis adhesion to TIGKs (** $P \leq 0.01$). Co-treatment with *L. acidophilus* at MOIs of 500, 1000, 2000 decreased *P. gingivalis* adhesion by 14%, 39%, and 52%, respectively. Overall, *L. acidophilus* pre-treatment resulted in a slightly greater reduction in *P. gingivalis* binding, relative to that observed for the same *L. acidophilus* co-treatment doses ($P > 0.05$).

(A)



(B)

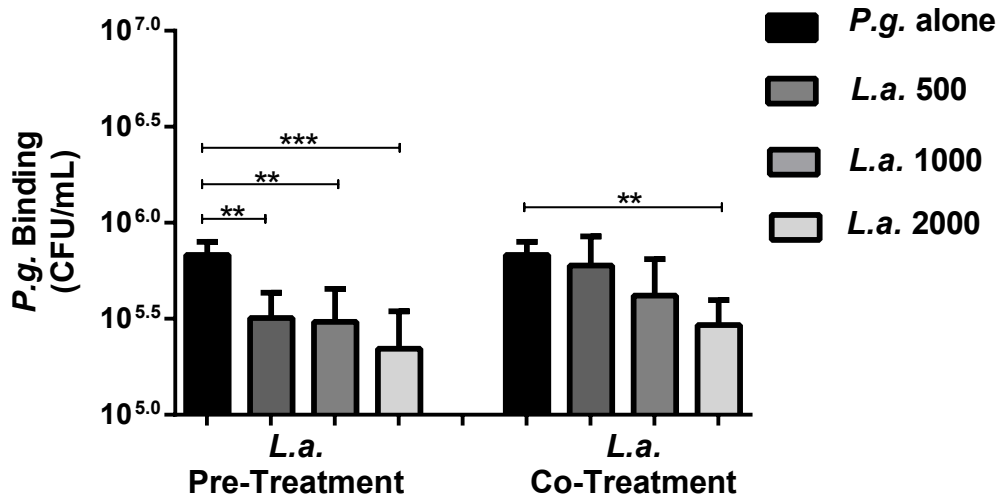


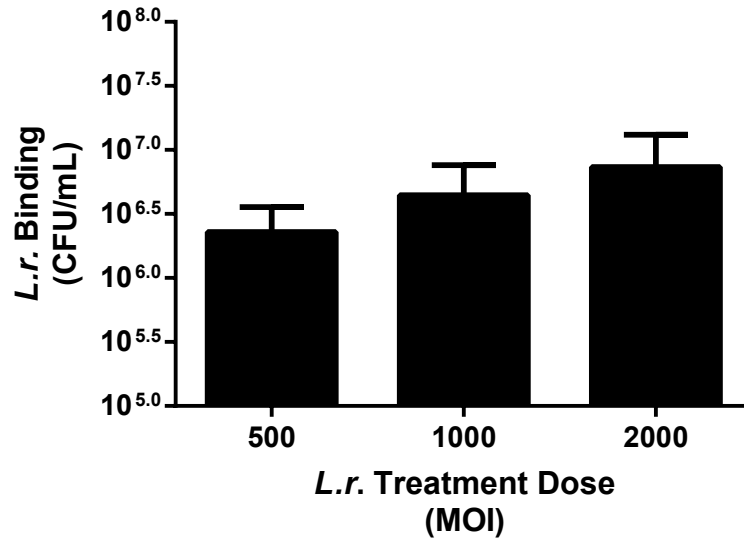
Figure 14: A. A dose-dependent trend in *L.a.* binding to TIGK cells is observed after administration of different *L.a.* MOI. TIGK cells, plated at a density of 1×10^5 cells per well, were treated with CS-labeled

L.a. at MOIs of 500, 1000, 2000 for 90 min. Values represent the mean \pm standard deviation of *L.a.* binding (CFU/mL) to TIGK cells at increasing MOIs. While a dose-dependent trend in binding was observed, increased binding was only observed between *L.a.* administered at low (MOI 500) and high concentrations (MOI 2000) (* $P \leq 0.05$). **B. Inhibition of *P.g.* adhesion to TIGK cells after different doses of pre- and co-treatment with *L.a.*** *L.a.* was applied to CS-labeled *P.g.* (MOI 2000)-treated TIGKs at MOIs of 500, 1000, 2000 for 90 min. Values represent the mean \pm standard deviation of *P.g.* adhesion (CFU/mL) to TIGK cells in the absence (*P.g.* alone) or presence of *L.a.* pre- or co-treatment. Statistical significance between *P.g.* alone and *L.a.*-treated groups was calculated by one-way ANOVA and is represented by ** $P \leq 0.01$, and *** $P \leq 0.001$. After pre-treatment, *L.a.* administered at all doses significantly inhibited *P.g.* binding to TIGK cells. For *L.a.* and *P.g.* co-treatment, *P.g.* inhibition was observed at the highest dose of *L.a.* (2000 MOI). Overall, *L.a.* pre-treatment resulted in a slightly higher reduction in *P.g.* binding, relative to that observed for the same *L.a.* co-treatment doses (* $P > 0.05$).

Free *L.r.* adheres to TIGK cells and reduces *P. gingivalis* adhesion to TIGK cells at an MOI of 500.

TIGK cells treated with different MOIs (500, 1000, and 2000) of *L. reuteri* demonstrated binding to TIGK cells; however, no statistical significance in binding was observed as a function of dose (**Figure 15A**, $P > 0.05$). Next, we evaluated the ability of free *L. reuteri*, administered as a pre- or co-treatment at MOIs of 500, 1000, and 2000, to inhibit *P. gingivalis* binding to TIGK cells (**Figure 15B**). Overall, pre-treatment of TIGKs with *L. reuteri* for 15 min at MOIs of 500, 1000, and 2000 reduced binding of *P. gingivalis* (MOI 2000) by 64%, 45%, and 63%, respectively. Statistical significance in the inhibition of *P. gingivalis* binding was only observed for *L. reuteri* administered at an MOI of 500 (* $P \leq 0.05$). Similarly, co-treatment with free *L. reuteri* at MOIs of 500, 1000, 2000 with *P. gingivalis* (MOI 2000) showed a trend in reducing *P. gingivalis* binding. Specifically, *L. reuteri* co-treatment decreased *P. gingivalis* binding by 23%, 40%, and 56% at respective MOIs of 500, 1000, and 2000. Overall, *L. reuteri* pre-treatment resulted in a similar reduction in *P. gingivalis* binding, relative to that observed for the same *L. reuteri* co-treatment doses ($P > 0.05$).

(A)



(B)

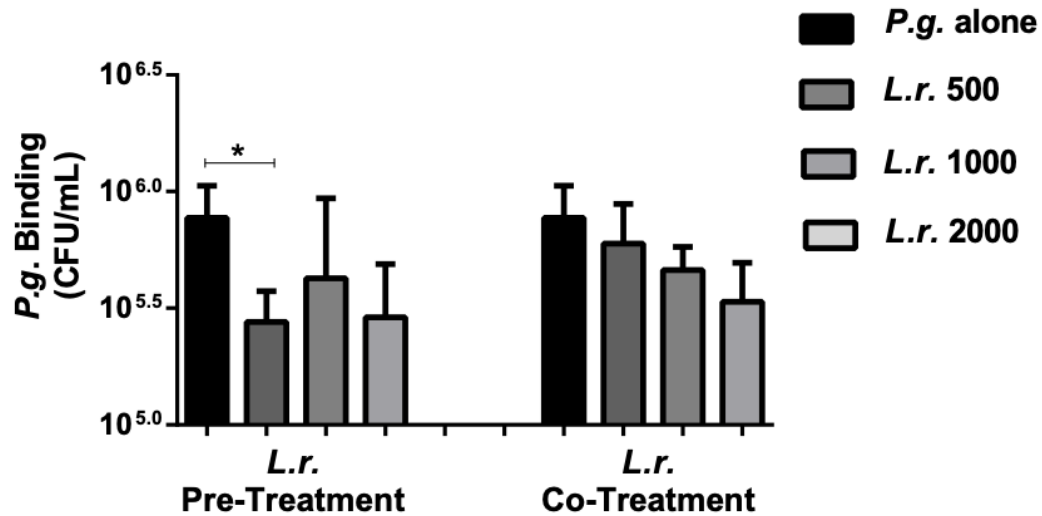


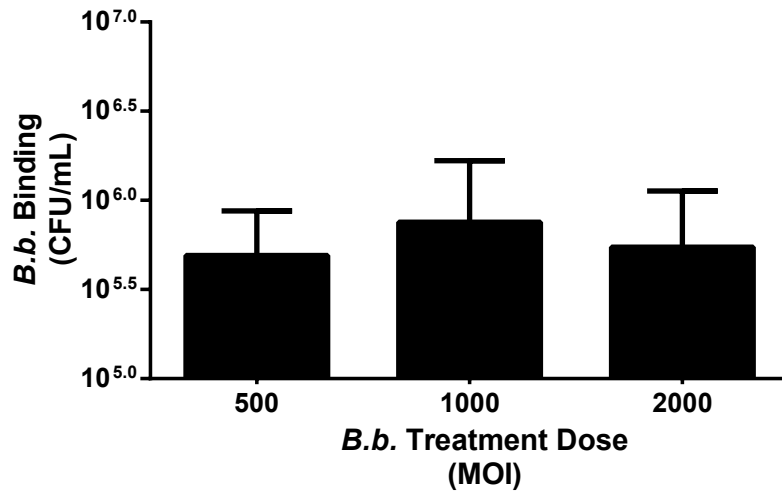
Figure 15: A. A dose-dependent trend in *L.r.* binding to TIGK cells is observed after administration of different *L.r.* MOI. TIGK cells plated at a density of 1×10^5 cells per well were treated with CS-labeled *L.r.* at MOIs of 500, 1000, 2000 for 90 min. Values represent the mean \pm standard deviation of *L.r.* binding (CFU/mL) to TIGK cells at increasing MOIs. While a dose-dependent trend in binding was observed, no statistical significance in binding was observed between different MOIs ($P > 0.05$). B. Inhibition of *P.g.* adhesion after different doses of pre- and co-treatment with *L.r.* *L.r.* was applied to CS-labeled *P.g.*

(MOI 2000)-treated TIGKs at MOIs of 500, 1000, 2000 for 90 min. Values represent the mean \pm standard deviation of *P.g.* adhesion (CFU/mL) to TIGK cells in the absence (*P.g.* alone) or presence of *L.r.* pre- or co-treatment. Statistical significance between *P.g.* alone and *L.r.*-treated groups was calculated by one-way ANOVA and is represented by * $P \leq 0.05$. No statistical significance was observed between *P.g.* alone and *L.r.*-pre- or co-treated groups, with the exception of *P.g.* and *L.r.* (500) pre-treatment. Overall, *L.r.* pre-treatment resulted in a similar reduction in *P.g.* binding, relative to that observed for the same *L.r.* co-treatment doses ($P > 0.05$).

Free *B.b.* adheres to TIGK cells and minimally impacts *P. gingivalis* adhesion to TIGK cells

TIGK cells treated with different MOIs (500, 1000, and 2000) of *B. bifidum* adhered to TIGK cells; however, no statistical significance or trend in binding, as a function of MOI, was observed (**Figure 16A**, $P > 0.05$). We further evaluated the ability of free *B. bifidum* administered as a pre- or co-treatment, to limit *P. gingivalis* binding to TIGK cells (**Figure 16B**). Pre-treatment of TIGKs with *B. bifidum* for 15 min at MOIs of 500, 1000, and 2000 reduced binding of *P. gingivalis* (MOI 2000) by 50%, 64%, and 79%, respectively. However, no statistical significance in *P. gingivalis* binding inhibition was observed at these MOIs ($P > 0.05$). Co-treatment with free *B. bifidum* at MOIs of 500, 1000, 2000 with *P. gingivalis* (MOI 2000) reduced *P. gingivalis* binding by 85%, 33%, and 50% at respective MOIs of 500, 1000, and 2000. Overall, *B. bifidum* pre-treatment resulted in a similar reduction in *P. gingivalis* binding, relative to that observed for the same *B. bifidum* co-treatment doses ($P > 0.05$).

(A)



(B)

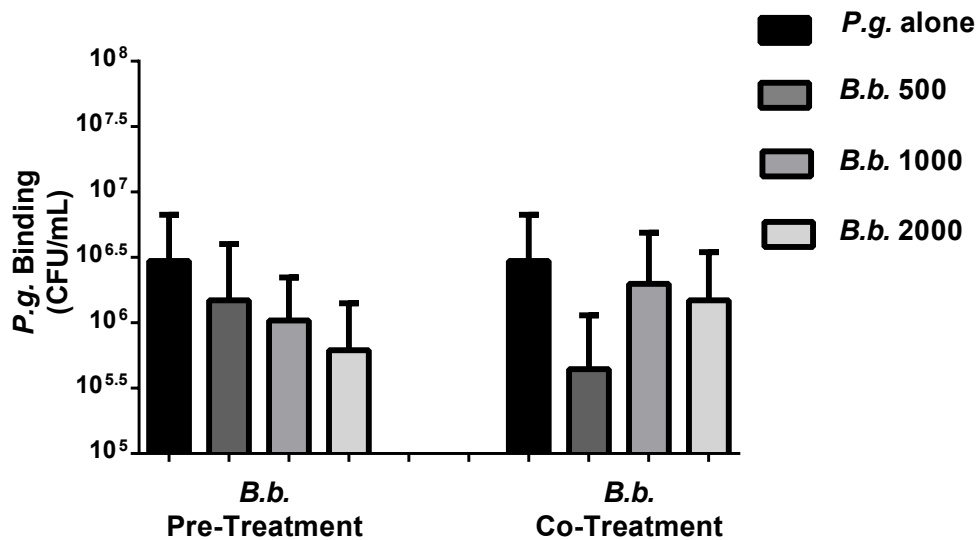


Figure 16: **A.** *B.b.* demonstrates binding to TIGK cells; however, no dose-dependence in adhesion is observed. TIGK cells, plated at a density of 1×10^5 cells per well, were treated with CS-labeled *B.b.* at MOIs of 500, 1000, 2000 for 90 min. Values represent the mean \pm standard deviation of *B.b.* binding (CFU/mL) to TIGK cells at increasing MOIs. Regardless of *B.b.* dose, similar binding was observed ($P > 0.05$). **B.** Inhibition of *P.g.* adhesion to TIGK cells after different doses of pre- and co-treatment with *B.b.* *B.b.* was applied to CS-labeled *P.g.* (MOI 2000)-treated TIGKs at MOIs of 500, 1000, 2000 for 90 min. Values

represent the mean \pm standard deviation of *P.g.* adhesion (CFU/mL) to TIGK cells in the absence (*P.g.* alone) or presence of *B.b.* pre- or co-treatment. Statistical significance between *P.g.* alone and *B.b.*-treated groups was calculated by one-way ANOVA. Both *P.g.* pre- and co-treatment, showed similar *P.g.* binding compared to the untreated control group ($P > 0.05$). Overall, *B.b.* pre-treatment resulted in a similar reduction in *P.g.* binding, relative to that observed for the same *B.b.* co-treatment doses ($P > 0.05$).

Examining *P. gingivalis* Invasion of TIGK Cells

P. gingivalis invasion of TIGK cells when administered at different doses

Next we evaluated the ability of *P. gingivalis*, administered at MOIs of 100, 500, 1000, and 2000 (corresponding to 1×10^7 , 5×10^7 , 1×10^8 , and 2×10^8 CFU/mL respectively), to invade TIGK cells (**Figure 17**). Overall, increased invasion of TIGKs was observed as a function of dose. *P. gingivalis* administered at a MOI of 2000 demonstrated increased levels of invasion, relative to *P. gingivalis* administered at an MOI of 100, 500, and 1000 (**** $P \leq 0.0001$).

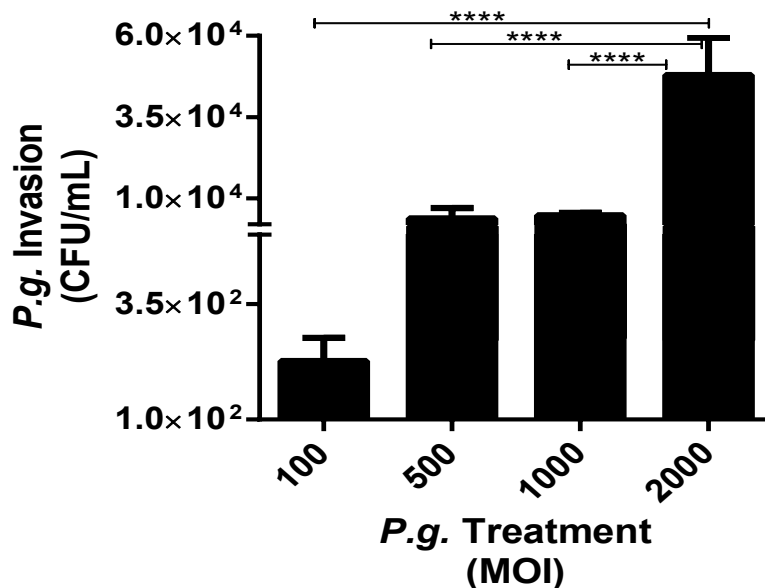


Figure 17: TIGK cells show a dose-dependent increase in *P. gingivalis* internalization. TIGK cells plated at a density of 1×10^5 cells per well were treated with *P.g.* at MOIs of 100, 500, 1000, 2000 for 90 min.

Antibiotics were subsequently administered to TIGK cells for 1 hr, followed by treatment with water for 20 min to lyse cells and enable the collection of internalized bacteria. The lysed fraction was plated on agar plates to determine the concentration (CFU/mL) of internalized bacteria. Values represent the mean \pm standard deviation of *P.g.* internalization (CFU/mL) in TIGK cells. Statistical significance in internalization as a function of administered *P.g.* dose was calculated by one-way ANOVA and is represented by ****P \leq 0.0001. At an MOI of 2000, *P.g.* internalization was significantly higher relative to *P.g.* administered at MOIs of 100, 500, 1000.

Results for TIGK Cell Viability Assay

Cell density determination for TIGK viability assay

Adhesion and invasion of *P. gingivalis* directly impacts the viability of GECs and affects tissue health. To evaluate the effect of probiotics on TIGK cell viability after *P. gingivalis* treatment, we performed an LDH cytotoxicity assay to assess LDH levels in TIGK cells after probiotic treatment. LDH secreted by TIGK cells is indicative of cytotoxicity caused by effector cells (here, *P. gingivalis*). To determine the appropriate TIGK cell plating density for this assay, LDH release from cells was evaluated at different TIGK cell densities (**Figure 18**). Free LDH provided by the manufacturer and unlysed/untreated TIGK cells served as positive and negative controls for LDH expression, respectively. Overall, a gradual increase in LDH response was found in both unlysed and lysed cells as cell density increased. Furthermore, as assay validation, a comparison of unlysed to lysed TIGK cells, plated at densities of 2.5×10^4 , 5×10^4 , 1×10^5 , and 2×10^5 , showed significantly higher levels of LDH expression, relative to similar density of unlysed TIGK cells (****P \leq 0.0001), which suggests that TIGK cells increase expression of LDH in the presence of adverse chemicals indicative of cytotoxicity. Cytotoxicity of the TIGK cells as measured by the LDH assay was proportional to the density of unlysed or lysed TIGK cells. A cell density of 5×10^4 was selected for further experiments as it produced the maximum difference in LDH release between unlysed and lysed cells.

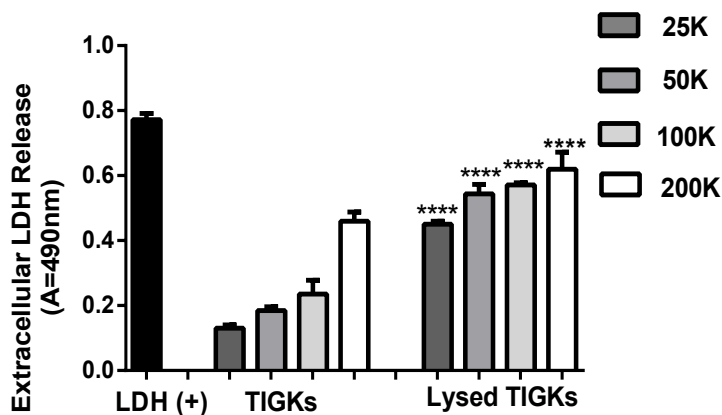


Figure 18: response between unlysed and lysed TIGK cells plated at different cell densities. LDH release from unlysed TIGK and lysed TIGK cells plated at densities of 2.5×10^4 , 5×10^4 , 1×10^5 , and 2×10^5 cells per well, was evaluated after 8 hr of incubation. Free LDH provided by the manufacturer and unlysed TIGK cells served as positive and negative controls for LDH expression, respectively. Values represent the mean \pm standard deviation of cell cytotoxicity, measured by assessing LDH release/activity as measured by production of a red formazan product at 490 nm. The statistical significance between unlysed and lysed TIGK cells plated at the same cell density was assessed by one-way ANOVA and is represented by **** $P \leq 0.0001$ between each group. The LDH response of lysed TIGK cells at all concentrations (2.5×10^4 , 5×10^4 , 1×10^5 , and 2×10^5) was significantly higher relative to the same density of unlysed TIGK cells.

LDH release (i.e. cytotoxicity) after treatment with different doses of *P. gingivalis*

TIGK cells plated at density of 50k were treated with different MOIs of *P. gingivalis* for 8 hr (**Figure 19**). Statistical significance in LDH release/cytotoxicity was observed after *P. gingivalis* administration at MOIs of 100, 500, and 1000, relative to untreated/unlysed TIGKs (** $P \leq 0.001$, **** $P \leq 0.0001$). This finding indicates that *P. gingivalis* induces cytotoxic effects on TIGK cells. Treatment with *P. gingivalis* at MOIs of 2500 and 5000 showed similar LDH release/cytotoxicity to untreated/unlysed TIGKs ($P > 0.05$).

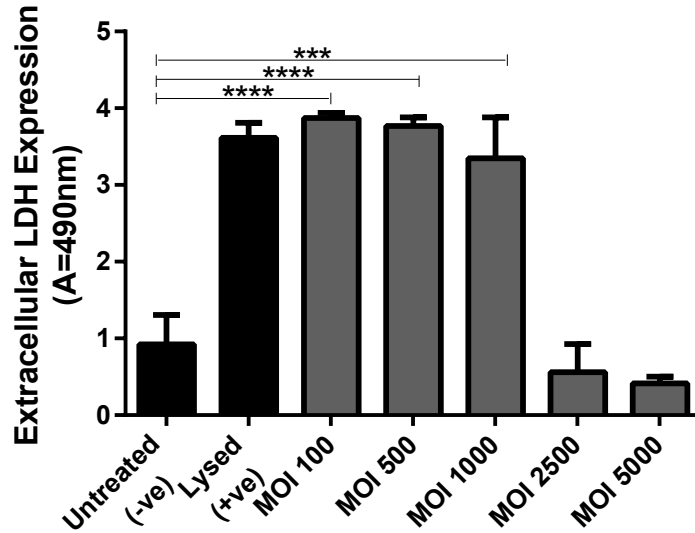


Figure 19: High levels of LDH release/cytotoxicity were observed after the administration of *P. gingivalis* at MOIs of 100, 500, and 1000. TIGK cells, plated at a density of 5×10^4 cells per well, were treated with *P.g.* at MOIs of 100, 500, 1000, 2500, 5000 for 8 hr. Untreated/unlysed TIGK cells and untreated/lysed TIGK cells served as negative and positive control groups for LDH production, respectively. Values represent the mean \pm standard deviation of cell cytotoxicity, measured by assessing LDH release/activity as measured by production of a red formazan product at 490 nm. Statistical significance was determined between untreated/unlysed and *P.g.*-treated cells, using one-way ANOVA and is represented by *** $P \leq 0.001$ and **** $P \leq 0.0001$. While higher MOIs of 2500 and 5000 show similar LDH response to untreated TIGK cells, lower MOIs of 100, 500, 1000 showed significantly higher LDH production relative to untreated/unlysed TIGK cells.

Specific Aim 2: Develop and characterize 3D-printed gelatin-alginate scaffolds that maximize probiotic viability and sustain the release of probiotics for ~7 to 14 days.

Our long-term goal for 3D-bioprinting was to develop a scaffold containing probiotics that is of suitable size and shape to place into a periodontal pocket after mechanical plaque removal or surgical periodontal procedure. These scaffolds were predicted to release probiotics sustainably for up to two weeks of periodontium healing. We envision that sustained delivery of probiotics at the desired (localized) site will

facilitate healing and periodontal health by decreasing colonization of pathogens and increasing beneficial probiotic accumulation in the oral cavity. At first we developed printing parameters suitable for a gelatin-alginate bioink and printed different scaffold shapes with the Allevi 3D printer. Figure 20 demonstrates various shapes of scaffolds created with the help of Allevi software demonstrating the ability to print a variety of structures with different morphological features suitable for different applications. Among these different patterns, we selected the 13x1 mm scaffold shown in Figure 20B, due to its suitable shape for subgingival pocket administration.

Development of 3D-bioprinted scaffold

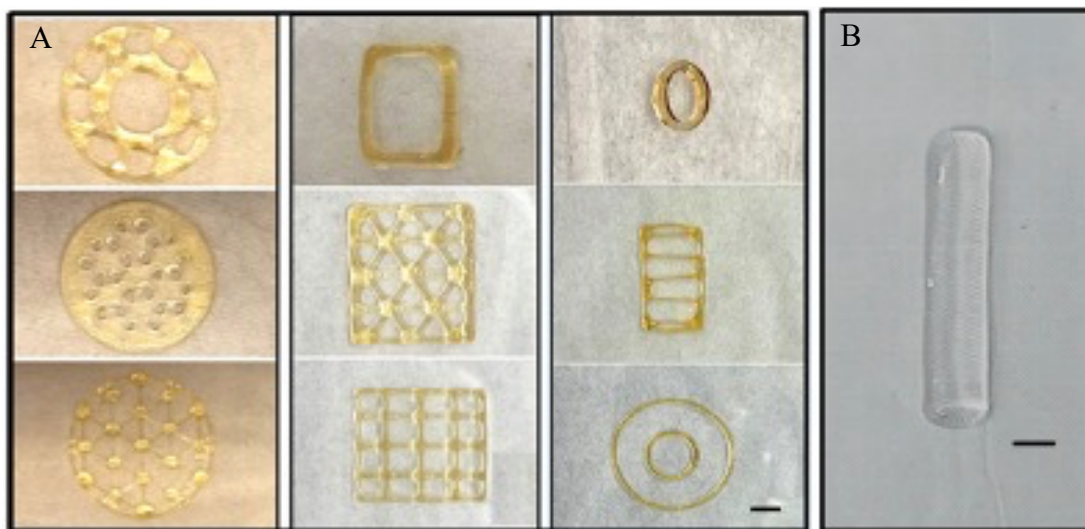


Figure 20: A. Different morphologies of 3D-bioprinted scaffolds demonstrate the ability to print scaffolds with various morphologies and dimensions, suitable for a variety of dental (and other) applications. B. Among these different patterns, the 13x1 mm scaffold was selected due to its suitable shape for subgingival pocket administration. Scale bar on left = 0.5 mm, right = 1 mm.

Evaluation of effects of printing conditions on bacterial cell viability

Bioprinting parameters such as temperature and pressure can affect bacterial cell viability post-printing. *L.a.* was incorporated at 5×10^7 CFU per mg polymer, and bacterial viability was assessed immediately post-printing (Figure 21). Overall, high probiotic viability was maintained during the printing process, with scaffolds demonstrating a high post-print viability of 1.1×10^7 CFU/mg – a loss of less than one logarithmic unit of bacteria during the printing process. Well maintained probiotic viability indicates the promising potential of 3D-bioprinting to incorporate high viable concentrations of probiotics.

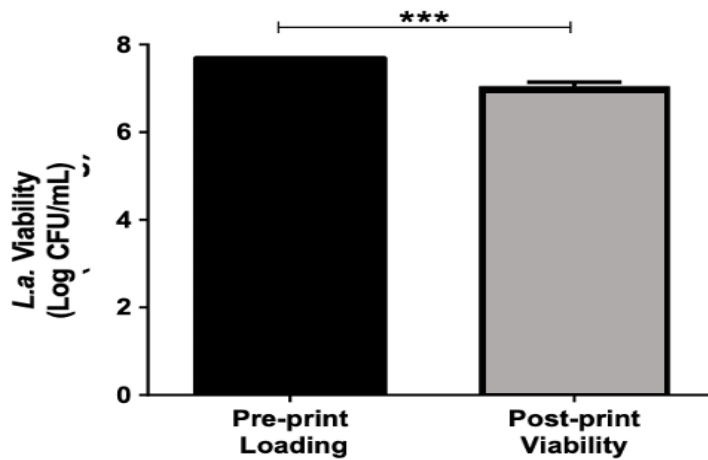


Figure 21. Probiotic viability was determined pre- and post-printing after initial incorporation of 5×10^7 CFU *L.a.* per mg scaffold. The concentration of *L.a.* added to the polymer solution prior to printing (5×10^7 CFU/mg) was considered as 100% viability. Post-print viability was determined by dissolving the scaffold in 1 mL MRS broth and plating aliquots of the scaffold dilutions on an agar plate. Values represent mean \pm standard deviation of CFU/mg post-printing. Overall *L.a.* viability decreased from 5×10^7 to 1.1×10^7 CFU/mg, showing less than a one-log decrease in probiotic viability (** $P \leq 0.001$).

L. acidophilus release from probiotic scaffolds

To demonstrate the potential of 3D-bioprinted scaffolds to sustain probiotic release in different media, we assessed the release kinetics of probiotics from scaffolds incubated in MRS broth, artificial saliva, and PBS

over 17 d (Figure 22). Release kinetics suggest that *L. acidophilus* incorporated in 3D scaffolds is released and likely proliferates for at least 14 days, suggesting the ability of 3D-bioprinted scaffolds to release bacteria within the desired timeframe of 7 to 14 d. Evaluation of release kinetics in MRS broth, artificial saliva, and PBS shows maximum release and proliferation of bacteria in MRS broth medium. In comparison, release in artificial saliva was detected after ~4 days incubation, while no *L. acidophilus* release was detected in PBS.

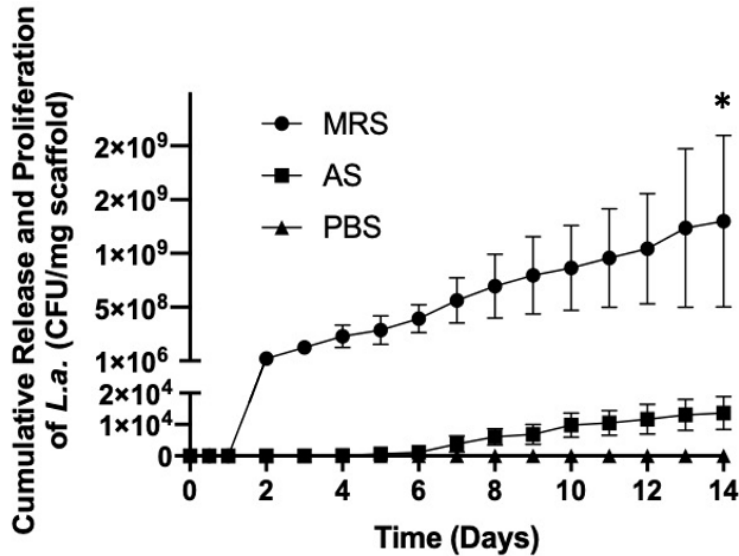


Figure 22. Cumulative release of *L.a.* from 3D-bioprinted scaffolds in PBS, MRS broth, and artificial saliva. *L.a.* concentration of 5×10^7 CFU/mg was added to 10% gelatin-2% alginate bioink and printed at 37°C and 42.5 psi. Bacterial release was assessed after 1 hr, 4 hr, and each day through 17 days in triplicates. Values indicate the mean \pm standard deviation of cumulative release of *L.a.* (CFU/mg) at each time point. Statistically significant release (and proliferation) of *L.a.* was found in MRS broth, relative to artificial saliva and PBS, after 14 days (* $P \leq 0.05$). *L.a.* release in artificial saliva and PBS was much lower relative to release in MRS broth. **Data in collaboration with Veeresh Rai, graduate student in Dr. Steinbach-Rankins Lab.

CHAPTER 5

DISCUSSION

Adhesion of *P. gingivalis* to gingival epithelial cells is the primary and most important mechanism for its colonization of the oral cavity. After initial attachment to the cell surface, with the help of major and minor fimbriae, *P. gingivalis* starts to auto- and co-aggregate with other bacteria such as *Actinomyces viscosus*, *Treponema denticola*, *Streptococcus gordonii*, and *Streptococcus oralis* [39-44]. This process facilitates accumulation of *P. gingivalis* and other bacteria in the oral cavity, leading to the initiation and progression of periodontal diseases. Furthermore, adhesion induces structural changes in the cell cytoskeleton that facilitates internalization of *P. gingivalis* [56, 58, 63]. Within the cytoplasm, internalized bacteria escape from the host immune surveillance and benefit from the nutrient-rich environment for their growth and proliferation. These nutrients and growth factors enable the bacteria to produce toxic metabolic products, compromising cell viability and leading to tissue destruction [59]. The invasion of *P. gingivalis* is also a major contributor to antibiotic and periodontal treatment failure, as internalized bacteria often recolonize the oral cavity post-treatment. Hence, bacterial adhesion and invasion are the important steps that eventually lead to disease progression and tissue destruction.

Among the potential biologics currently available to treat pathogen-mediated oral diseases, probiotics seem quite promising. Probiotics have been effective in the treatment of many GI disorders, *H. pylori* infection, and skin and vaginal infections because of their ability to reduce pathogen adhesion [80-82]. *However, to date, no in vitro studies have evaluated the potential of probiotics to reduce oral pathogen adhesion, invasion and subsequent killing of host cells. Hence, this study aimed to assess the beneficial properties of different probiotics against a major periodontal pathogen, P. gingivalis.* Adhesion, antibiotic protection and LDH cytotoxicity assays were conducted to evaluate the effects of probiotic administration on *P. gingivalis* adhesion to and invasion of TIGK cells, and on modulating TIGK cell viability.

Unlike previous studies that evaluated probiotics for systemic applications, this study provides important insight into specific probiotics species effectiveness against a prominent oral pathogen, *P. gingivalis*. It evaluates the previous theories of probiotic mechanisms and provides evidence that probiotics can adhere to and potentially interfere with *P. gingivalis* binding. Furthermore, the development and characterization of scaffolds fabricated with 3D-bioprinting may help to overcome the limitations of current approaches and provide a novel therapeutic avenue for the future prevention and treatment of periodontitis.

In these studies we observed that treatment with *L. acidophilus*, *L. reuteri*, or *B. bifidum* alone resulted in probiotic adhesion to TIGK cells. These observations suggested that probiotics may occupy adhesion sites on the host surface, and may thereby decrease potential binding sites for pathogen attachment, resulting in reduced pathogen adhesion. However, when TIGK cells were pre- or co-treated with *L. acidophilus*, *L. reuteri*, or *B. bifidum* in conjunction with *P. gingivalis*, only pre-treatment with *L. acidophilus* (and one concentration of co-treatment) demonstrated a statistically significant decrease in *P. gingivalis* adhesion to TIGK cells. Pre-treatment with *L. acidophilus* at all MOIs (500, 1000, 2000) and co-treatment with an MOI of 2000 showed a statistically significant reduction in adhesion suggesting *L. acidophilus* as a promising probiotic to limit *P. gingivalis* adhesion. Furthermore, relative to co-treatment, *L. acidophilus* pre-treatment seemed to enhance the inhibition of *P. gingivalis* adhesion. These observations support the hypothesis that a reduction in pathogen colonization can be attained and potentially attributed to enhanced probiotic binding to TIGK cell adhesion sites, relative to *P. gingivalis*. Pre-treatment with probiotics such as *L. acidophilus*, may enable probiotics to preoccupy the binding sites commonly sought by *P. gingivalis*, leading to decreased availability of adhesion sites and reduced bacterial adhesion. These findings suggest the potential of *L. acidophilus*, and potentially other probiotics, administered after mechanical debridement (prior to subsequent pathogen colonization), to delay or reduce the bacterial recolonization. Furthermore, these data suggest that pre-administration may be more efficacious, than administration at later times, potentially due to the mechanism by which probiotics occupy binding sites and prevent pathogen binding on eukaryotic cells.

While a comparison of data collected to date, with *L. acidophilus*, *L. reuteri*, and *B. bifidum* pre-treatment indicates that *L. acidophilus* may be the most effective probiotic species to reduce *P. gingivalis* adhesion,

future work would benefit from varying the dose of *P. gingivalis* to assess its impact on probiotic adhesion and subsequent inhibition.

In parallel with evaluating the potential of *P. gingivalis* to bind to TIGK cells in the presence or absence of probiotics, results from the antibiotic protection assay indicate that *P. gingivalis* invasion of TIGK cells exhibits some level of dose-dependence – highlighting the importance of mitigating *P. gingivalis* adhesion to TIGK cells. After this initial experiment, several trials of the antibiotic protection assay were performed after pre- and co-treatment with *L. acidophilus*, *L. reuteri*, or *B. bifidum* following the same protocols. However, these experiments were difficult to evaluate. We found similar clustered colonies of *P. gingivalis* and probiotics together for pre- and co-treatment groups on agar plates, making them difficult to distinguish because of similar appearance. To overcome this challenge, we incorporated an inhibitory concentration (0.5 µg/ml) of streptomycin in our agar plate to prevent probiotic colony formation in pre- and co-treatment groups. However, the addition of streptomycin decreased the viability of both pre and co- cultures on agar plates. Similarly, free probiotics and the *P. gingivalis* group also showed decreased viability on streptomycin modified agar plates. These findings suggest that the concentration of antibiotics is too high, and may kill the relatively small amount of invaded bacteria, thereby preventing colony formation on agar plates. Future experiments may be conducted to assess the appropriate dose of antibiotics to kill probiotics and enable only *P. gingivalis* growth on the agar plates. Additionally, these challenges may be overcome by using a *P. gingivalis* strain that is capable of encoding beta lactase enzymes, which provide bacterial resistance to antibiotics. Use of an antibiotic-resistant *P. gingivalis* strain may help to facilitate its growth on antibiotic-treated agar plates to enable the evaluation of its invasion in the presence of probiotics. Additionally, other methods including phase contrast and confocal microscopy should be adopted to evaluate *P. gingivalis* internalization in different treatment groups.

Additionally, we performed an LDH cytotoxicity assay to evaluate the effects of *P. gingivalis* on TIGK cell viability both with and without probiotic application. We first performed the LDH assay with different plating densities of TIGK cells to ensure observation of LDH production in lysed cells and that the assay was working properly. As anticipated, an increase in LDH release was seen in the lysed, relative to the unlysed cell group.

Among the plated cell densities (25k, 50k, 100k, and 200k cells per well), a maximum difference between lysed and unlysed groups was observed at a density of 50k cells (after 8 hr incubation). Using this information, subsequent experiments were conducted to evaluate LDH response after treatment with *P. gingivalis* at MOIs of 100, 500, 1000, 2500, 5000 to determine the appropriate MOI for future experiments with probiotics. After treatment with lower MOIs of 100, 500, and 1000 *P. gingivalis*, a significant increase in LDH release was observed. In contrast, higher MOIs of 2500 and 5000 resulted in LDH release similar to untreated/unlysed cells. Future experiments will be conducted to reassess the impact of higher MOIs and different durations of incubation on LDH expression.

In addition to adhesion, invasion, and cell viability studies, in future work, we would like to evaluate the effects of probiotics on *P. gingivalis*-mediated enhanced cytokine response. We aim to determine modulation in IL-8 and TNF cytokine levels with the help of ELISA after probiotic administration. Results from these studies will provide valuable insight regarding the role probiotics play in improving *P. gingivalis*-mediated inflammation.

Aerobic and anaerobic probiotic species such as *L. paracasei*, *L. rhamnosus*, *L. salivarius*, and *Bifidobacteria* are found in the healthy oral cavity and contribute to 1% of the total microflora, suggesting the ability of probiotics to survive and grow in the oral environment. A variety of delivery vehicles, including nanoparticles and fibers have been used to deliver active agents to the oral cavity. However, nanoparticles and fibers have certain limitations, which include harsh processing conditions, limited architectural features, burst release of incorporated agents, and complex fabrication techniques. These limitations may be overcome by using a novel 3D-bioprinting approach that highly incorporates viable probiotics using a variety of biocompatible materials. Overall, 3D-bioprinting is less technique-sensitive and potentially more efficient, due to its ability to highly incorporate live cells and release incorporated agents for longer durations.

In this work, 3D-bioprinting of probiotics with gelatin alginate bioinks produced structurally stable scaffolds. Post-print crosslinking enhanced the mechanical properties and increased the duration of scaffold stability (demonstrated via release). However, high printing temperature and pressure may impact probiotic viability.

To evaluate these effects, we compared probiotic viability before and after printing, recovering 1.1×10^7 bacteria. Less than a one-log decrease in bacterial viability indicates that 3D-bioprinting with an extrusion-based technique provides a promising approach by which to incorporate and maintain the viability of live prokaryotic cells in a scaffold. Evaluation of release kinetics in MRS broth, PBS, and artificial saliva showed the preliminary potential of 3D-bioprinted scaffolds to gradually release and foster the proliferation of probiotics over 14 days. Compared to probiotic release in PBS and artificial saliva, MRS broth provided high levels of *L. acidophilus* release and proliferation of *L. acidophilus*. Artificial saliva showed comparatively lesser release of probiotics relative to that observed in MRS broth. These findings may be due to the overall lower concentration of glucose in artificial saliva relative to MRS. Due to the low probiotic viability seen in artificial saliva, future work may want to investigate other artificial salivas with higher glycogen content, used for pharmaceutical testing.

Previous work in our group has focused on increasing the retention of delivery vehicles in the oral cavity with a variety of surface modifications [177, 178]. Similarly we could use chitosan or other adhesives to enhance mucoadhesion of the scaffolds in subgingival pockets [179]. However, current results indicate that 3D-bioprinting addresses previously mentioned limitations of nano particles and fibers. In contrast to these dosage forms, 3D-bioprinting excludes the use of harmful solvents in formulating the delivery vehicle, thereby preserving the viability of active biologics. 3D-bioprinted scaffolds also possess enhanced geometric diversity and structural stability compared to nanofibers. Release results from our study show that probiotic release from scaffolds is sustained up to 14 days, which may, in the right environment, overcome the limitation of burst release from other dosage forms.

Future experiments will seek to evaluate these scaffolds *in vitro* to assess their ability to reduce *P. gingivalis* adhesion to and invasion of TIGK cells similar to free probiotics. Following that, the aim will be to evaluate these scaffolds *in vivo*. We desire to utilize either a ligature-induced periodontitis model or Baker model to test these scaffolds for efficacy against periodontitis in *in vivo* studies. The ligature-induced periodontitis model uses silk ligature to induce periodontitis and alveolar bone loss in mice. A ligature is tied in the gingival sulcus commonly around the maxillary second molar which helps to gain reproducibility and increase validity [180]. The ligature facilitates bacterial plaque accumulation and causes inflammation [180-182]. This model

is considered advantageous because of its predictability of events and duration for causing periodontitis and alveolar bone loss [181-184]. Another model is the Baker model in which mice are infected orally with *P. gingivalis*, causing periodontitis and alveolar bone loss [185]. This model allows for controlled environmental conditions in which mice naturally develop periodontitis over a period of time identical periodontitis in humans [186].

Results from these future studies would lend further support to the idea that probiotics administered in 3D-bioprinted scaffolds, after mechanical plaque removal or surgical periodontal procedures, can be an effective strategy to combat recolonization of *P. gingivalis* in the oral cavity during healing. The aim will be to utilize these scaffolds for two weeks following periodontal treatment by placing it in subgingival pockets and ensuring its retention with the help of adhesives. Sustained release of probiotics in subgingival pockets will help to reduce recolonization of pathogens in diseased site and provide beneficial effects during the healing period, improving the outcomes of periodontal interventions.

REFERENCES

1. Graves DT., Jiang Y., et al., Periodontal disease: bacterial virulence factors, host response, and impact on systemic health. *Current Opinion in Infectious Diseases*, 2000. 13(3): p. 227-32.
2. Eke PI., Dye BA., et al., Update on prevalence of periodontitis in adults in the United States: NHANES 2009 to 2012. *Journal of Periodontology*, 2012. 86(5): p. 611-22.
3. Listl S., Galloway J., et al., Global economic impact of dental diseases. *J Dent Res*, 2015. 94(10): p. 1355-61.
4. Kassebaum NJ., Smith AGC., et al., Global, regional, and national prevalence, incidence, and disability- adjusted life years for oral conditions for 195 countries, 1990–2015: A systematic analysis for the global burden of diseases, injuries, and risk factors. *Journal of Dental Research*, 2017. 96(4): p. 380-7.
5. Tonetti MS., Greenwell H., et al., Staging and grading of periodontitis: Framework and proposal of a new classification and case definition. *J Periodontol*, 2018. 89(S1): p. 159-72.
6. Chapple ILC., Mealey BL., et al., Periodontal health and gingival diseases and conditions on an intact and a reduced periodontium: consensus report of workgroup 1 of the 2017 world workshop on the classification of periodontal and peri-implant diseases and conditions. *Journal of Periodontology*, 2018. 89(1): p. 74-84.
7. Diaz PI., Strausbaugh LD., et al., Fungal-bacterial interactions and their relevance to oral health: linking the clinic and the bench. *Front Cell Infect Microbiol*, 2014. 4: p. 101
8. Marsh PD., Zaura E., Dental biofilm: ecological interactions in health and disease. *J Clin Periodontol*, 2017. 44(18): p.12-22.
9. Abranches J., Zeng L., et al., Biology of oral *Streptococci*. *Microbiol Spectr*, 2018. 6(5).
10. Diaz PI., Chalmers NI., et al., Molecular characterization of subject-specific oral microflora during initial colonization of enamel. *Appl Environ Microbiol*, 2006. 72(4): p. 2837-48.
11. Nyvad B., Kilian M., Microbiology of the early colonization of human enamel and root surfaces in vivo. *Scand J Dent Res*, 1987. 95(5): p. 369-80.
12. Heim KP., Sullan RMA., et al., Identification of a supramolecular functional architecture of *Streptococcus mutans* adhesin P1 on the bacterial cell surface. *J Biol Chem*, 2015. 290(14): p. 9002-19.
13. Takahashi Y., Konishi K., et al., Identification and characterization of hsa, the gene encoding the sialic acid-binding adhesin of *Streptococcus gordonii* DL1. *Infect Immun*, 2002. 70(3): p.1209-18.
14. Cisar JO., Barsumian EL., et al., Immunochemical and functional studies of *Actinomyces viscosus* T14V type 1 fimbriae with monoclonal and polyclonal antibodies directed against the fimbrial subunit. *J Gen Microbiol*, 1991. 137(8): p.1971-9.
15. Rosan B., Lamont RJ., Dental plaque formation. *Microbes Infect*, 2000. 2(13): p.1599-607.
16. Marsh PD., Dental plaque as a biofilm and a microbial community implication for health and disease. *BMC Oral Health*, 2006. 6(1): p.1-14.
17. Kolenbrander PE., Palmer RJ., et al., Oral multispecies biofilm development and the key role of cell-cell distance. *Nat Rev Microbiol*, 2010. 8(7): p. 471-80.
18. Mazumdar V., Amar S., et al., Metabolic proximity in the order of colonization of microbial community. *PLOS One*, 2013. 8(10): p. 7761.
19. Roberts AP., Kreth J., The impact of horizontal gene transfer on the adaptive ability of the human oral microbiome. *Front Cell Infect Microbiol*, 2014. 4: p. 124.
20. Flemming HC., Wingender J., et al., Biofilms: an emergent form of bacterial life. *Nat Rev Microbiol*, 2016.14(9): p. 563-75.
21. Kaplan JB., Biofilm dispersal, mechanisms, clinical implications, and potential therapeutic uses. *J Dent Res*. 2010. 89(3): p. 205–18.

22. Choi YC., Morgenroth E., Monitoring biofilm detachment under dynamic changes in shear stress using laser-based particle size analysis and mass fractionation. *Water Sci Technol*, 2010. 47: p. 69-76.
23. Lawrence JR., Scharf B., et al, Microscale evaluation of the effects of grazing by invertebrates with contrasting feeding modes on river biofilm architecture and composition. *Microb Ecol*, 2002. 44: p. 199-207.
24. Ymele-Leki P., Ross JM., Erosion from *Staphylococcus aureus* biofilms grown under physiologically relevant fluid shear forces yields bacterial cells with reduced avidity to collagen. *Appl Environ Microbiol*, 2007. 73: p. 1834-41.
25. Erard JC., Miyasaki KT., et al., Detachment of oral bacteria from saliva-coated hydroxyapatite by polymorphonuclear leukocytes. *J Periodontol*, 1989. 60: p. 211-6.
26. Socransky SS., Haffajee AD., et al., Microbial complexes in subgingival plaque. *J Clin Periodontol*, 1998. 25(2): p. 134-44.
27. da Silva-Boghossian CM., do Souto RM., et al., Association of red complex, *A. actinomycetemcomitans* and non-oral bacteria with periodontal diseases. *Arch Oral Biol*, 2011. 56(9): p. 899-906.
28. Suzuki N., Yoneda M., et al., Mixed red-complex bacterial infection in periodontitis. *Int J Dent*, 2013. p. 587279.
29. Yost S., Duran-Pinado A., et al., Functional signatures of oral dysbiosis during periodontitis progression revealed by microbial metatranscriptome analysis. *Genome Med*, 2015. 7(1): p. 27.
30. Hajishengallis G., Lamont RJ., Beyond the red complex and into more complexity: the Polymicrobial Synergy and Dysbiosis (PSD) Model of periodontal disease etiology. *Mol Oral Microbiol*, 2012. 27(6): p. 409-19.
31. Lamont RJ., Koo H., et al., The oral microbiota: dynamic communities and host interactions. *Nat Rev Microbiol*, 2018. 16(12): p. 745-59.
32. Hajishengallis G., Liang S., et al., Low abundance biofilm species orchestrates inflammatory periodontal disease through the commensal microbiota and complement. *Cell Host Microbe*, 2011. 10: p. 497-506.
33. Hajishengallis G., Lamont RJ., Breaking bad: Manipulation of the host response by *Porphyromonas gingivalis*. *Eur J Immunol*, 2014. 44(2): p. 328-38.
34. How KY., Song KP., et al., *Porphyromonas gingivalis*: An overview of periodontopathic pathogen below the gum line. *Frontiers in microbiology*, 2016. 7: p. 53.
35. Hajishengallis G., Liang S., et al., Low-abundance biofilm species orchestrates inflammatory periodontal disease through the commensal microbiota and complement. *Cell Host Microbe*, 2011. 10(5): p. 497-506.
36. Di Benedetto A., Gigante I., et al., Periodontal disease: linking the primary inflammation to bone loss. *Clinical and Developmental Immunology*, 2013. 2013: p. 7.
37. Graves DT., Cochran D., The contribution of interleukin-1 and tumor necrosis factor to periodontal tissue destruction. *J Periodontol*, 2003. 74(3): p. 391- 401.
38. Enersen M., Nakano K., et al., *Porphyromonas gingivalis* Fimbriae. *J Oral Microbiol*, 2013. 5: p. 1-10.
39. Kuboniwa M., Amano A., et al., Homotypic biofilm structure of *Porphyromonas gingivalis* is affected by fimA type variations. *Oral Microbiol Immunol*, 2009. 24: p. 260-3.
40. Kuboniwa M., Amano A., et al., Distinct roles of long/short fimbriae and gingipains in homo-typic biofilm development by *Porphyromonas gingivalis*. *BMC Microbiol*, 2009. 9: p.105.
41. Goulbourne PA., Ellen RP., Evidence that *Porphyromonas* (Bacteroides) *gingivalis* fimbriae function in adhesion to *Actinomyces viscosus*. *J Bacteriol*, 1991. 173: p. 5266-74.
42. Hashimoto M., Ogawa S., et al., Binding of *Porphyromonas gingivalis* fimbriae to *Treponema Denticola* dentilisin. *FEMS Microbiol Lett*, 2003. 226: p. 267-71.
43. Lamont RJ., Bevan CA., et al., Involvement of *Porphyromonas gingivalis* fimbriae in adherence to *Streptococcus gordonii*. *Oral Microbiol Immunol*, 1993. 8: p. 272-6.
44. Maeda K., Nagata H., et al., Glyceraldehyde-3-phosphate dehydrogenase of *Streptococcus oralis* functions as a coadhesin for *Porphyromonas gingivalis* major fimbriae. *Infect Immun*, 2004. 72: p. 1341-8.
45. Hamada N., Watanabe K., et al., Construction and characterization of a fimA mutant of *Porphyromonas gingivalis*. *Infect Immun*, 1994. 62: p.1696-704.

46. Andrian E., Grenier D., et al., *Porphyromonas gingivalis*-epithelial cell interactions in periodontitis. *J Dent Res*, 2006. 85: p.392–403.
47. Park Y., Simionato MR., et al., Short fimbriae of *Porphyromonas gingivalis* and their Role in coadhesion with *Streptococcus gordonii*. *Infect Immun*, 2004.73: p. 3983-9.
48. Wang B., Wu J., et al., Negative correlation of distributions of *Streptococcus cristatus* and *Porphyromonas gingivalis* in subgingival plaque. *J Clin Microbiol*, 2009. 47: p. 3902–6.
49. Dixon DR., Darveau RP., Lipopolysaccharide heterogeneity: innate host responses to bacterial modification of lipid a structure. *J Dent Res*, 2005. 84: p. 584–95.
50. Nakao R., Senpuku H., et al., *Porphyromonas gingivalis* galE is involved in lipopolysaccharide O-antigen synthesis and biofilm formation. *Infect Immun*, 2006. 74: p. 6145–53.
51. Capestany CA., Kuboniwa M., et al., Role of the *Porphyromonas gingivalis* InlJ protein in homotypic and heterotypic biofilm development. *Infect Immun*, 2006. 74: p. 3002–5.
52. Davey ME., Duncan MJ., Enhanced biofilm formation and loss of capsule synthesis: Deletion of a putative glycosyltransferase in *Porphyromonas gingivalis*. *J Bacteriol*, 2006.188: p. 5510–23.
53. Rosen G., Sela MN., Coaggregation of *Porphyromonas gingivalis* and *Fusobacterium nucleatum* PK 1594 is mediated by capsular polysaccharide and lipopolysaccharide. *FEMS Microbiol Lett*, 2006. 256: p. 304–10.
54. Ewanowich CA., Melton AR., et al., Invasion of HeLa 229 cells by virulent *Bordetella pertussis*. *Infect. Immun*, 1989. 57: p. 2698–704.
55. Gerits E., Verstraeten N., et al., New approaches to combat *Porphyromonas gingivalis* biofilms. *Journal of Oral Microbiology*, 2017. 9(1): p. 1300366.
56. Finlay BB., Falkow S., Common themes in microbial pathogenicity. *Microbiol. Rev*, 1989. 53(2): p. 210–30.
57. Gaillard JL., Berche P., et al., In vitro model of penetration and intracellular growth of *Listeria monocytogenes* in the human enterocyte-like cell line Caco-2. *Infect. Immun*, 1987. 55(11): p.2822–9.
58. Falkow S., Bacterial entry into eucaryotic cells. *Cell*, 1991. 65(7): p.1099–102.
59. Lamont RJ., Oda D., et al., Interaction of *Porphyromonas gingivalis* with gingival epithelial cells maintained in culture. *Oral Microbiol. Immunol*, 1992.7(6): p.364–7.
60. Lamont RJ., Chan A., et al., *Porphyromonas gingivalis* invasion of gingival epithelial cells. *Infection And Immunity*, 1995. 63(10): p. 3878–85.
61. Sandros J., Papapanou PN., et al., *Porphyromonas gingivalis* invades human pocket epithelium *in vitro*. *J. Periodontal Res*, 1994. 29(1): p. 62–9.
62. Sansonetti PJ., Bacterial pathogens, from adherence to invasion: Comparative strategies. *Med. Microbiol. Immunol*, 1993.182(5): p. 223–32.
63. Rosenshine I., Finlay BB., Exploitation of host signal transduction pathways and cytoskeletal functions by invasive bacteria. *BioEssays*, 1993. 15(1): p.17–24.
64. Bliska JB., Galan JE., et al., Signal transduction in the mammalian cell during bacterial attachment and entry. *Cell*, 1993. 73(5): p. 903–20.
65. Gaffen SL., Hajishengallis G., A new inflammatory cytokine on the block: Re-thinking periodontal disease and the Th1/Th2 paradigm in the context of Th17 cells and IL-17. *J Dent Res*, 2008. 87(9): p. 817-28.
66. Prakasam A., Elavarasu SS., et al., Antibiotics in the management of aggressive periodontitis. *J Pharm Bioallied Sci*, 2012. 4(2): p. 252–5.
67. Herrera D., Sanz M., et al., A systematic review on the effect of systemic antimicrobials as an adjunct to scaling and root planing in periodontitis patients. *J Clin Periodontol*, 2002. 29(3): p.136–59.
68. Xajigeorgiou C., Sakellari D., et al, Clinical and microbiological effects of different antimicrobials on generalized aggressive periodontitis. *J Clin Periodontol*, 2006. 33(4): p. 254–64.
69. Kapoor A., Malhotra R., et al., Systemic antibiotic therapy in periodontics. *Dent Res J (Isfahan)*, 2012. 9(5): p. 505–15.
70. Heitz-Mayfield LJ., Mombelli A., The therapy of periimplantitis: a systematic review. *Int J Oral Maxillofac Implants*, 2014. 29: p. 325–45.
71. Keestra JA., Grosjean I., et al., Non-surgical periodontal therapy with systemic antibiotics in patients with untreated aggressive periodontitis: a systematic review and meta-analysis. *J Periodontal Res*, 2015. 50(3): p.689–706.

72. Slots J., Ting M., Systemic antibiotics in the treatment of periodontal diseases. *Periodontol*, 2002. 28: p. 106–76.
73. Maezono H., Noiri Y., et al., Antibiofilm effects of azithromycin and erythromycin on *Porphyromonas gingivalis*. *Antimicrob Agents Chemother*, 2011. 55(12): p. 5887–92.
74. Saini R., Saini S., et al., Biofilm: A dental microbial infection. *J Nat Sci Biol Med*, 2011. 2(1): p. 71-5.
75. Kalia VC., Quorum sensing inhibitors: an overview. *Biotechnol Adv*, 2013. 31(2): p. 224–45.
76. Jang YJ., Choi YJ., et al., Autoinducer 2 of *Fusobacterium nucleatum* as a target molecule to inhibit biofilm formation of periodontopathogens. *Arch Oral Biol*, 2013. 58(1): p. 17–27.
77. Cho YJ., Song HY., et al., In vivo inhibition of *Porphyromonas gingivalis* growth and prevention of periodontitis with quorum-sensing inhibitors. *J Periodontol*, 2016. 87(9): p. 1075–82.
78. Metchnikoff E., *The prolongation of life: Optimistic studies*. London: Springer Publishing Company, 1906. p. 1–294.
79. Joint FAO/WHO working group report on drafting guidelines for the evaluation of probiotics in food. London, Ontario, Canada; 2002; April 30 and May 1. de Vrese M, Schrezenmeir J. Probiotics, prebiotics, and synbiotics. *Adv Biochem Eng Biotechnol* 2008;111:1-66.
80. Saxelin M., Tynkkynen S., et al., Probiotic and other functional microbes: from markets to mechanisms. *Curr Opin Biotechnol*, 2005. 16(2): p. 204-11.
81. Haukioja A., Probiotics and oral health. *Eur J Dent*, 2010. 4(3): p. 348-55.
82. Geier MS., Butler RN., et al., Inflammatory bowel disease: current insights into pathogenesis and new therapeutic options; probiotics, prebiotics and synbiotics. *Int J Food Microbiol*, 2007. 115(1): p. 1-11.
83. Patil MB., Reddy N., Bacteriotherapy and probiotics in dentistry. *KSDJ*, 2006. 2: p. 98-102.
84. Elisa KB., Scott BS., Regulatory T cells in IBD. *Curr Opin Gastroenterol*, 2008. 24: p.733-41.
85. Manisha N., Ashar et al., Role of probiotic cultures and fermented milk in combating blood cholesterol. *Indian J Microbial*, 2001. 41: p. 75-86.
86. Marco ML., Pavan S., et al. Towards understanding molecular modes of probiotic action. *Curr Opin Biotechnol*, 2006. 17(2): p. 204-10.
87. Volozhin AI., Il'in VK., et al., Development and use of periodontal dressing of collagen and *Lactobacillus casei* cell suspension in combined treatment of periodontal disease of inflammatory origin (a microbiological study). *Stomatologia(Mosk)*, 2004. 83(6): p. 6-8.
88. Tsubura S., Mizunuma H., et al, The effect of *Bacillus subtilis* mouth rinsing in patients with periodontitis. *Eur J Clin Microbiol Infect Dis*, 2009. 28(11): p. 1353-6.
89. Shimauchi H., Mayanagi G., et al, Improvement of periodontal condition by probiotics with *Lactobacillus salivarius* WB21; a randomized, double-blind, placebocontrolled study. *J Clin Periodontal*, 2008. 35(10): p. 897-905.
90. Della Riccia DN., Bizzini F., et al., Anti-inflammatory effects of *Lactobacillus brevis*(DC2) on periodontal disease. *Oral Dis*, 2007. 13(4): p. 376-85.
91. Staab B., Eick S., et al., The influence of a probiotic milk drink on the development of gingivitis: a pilot study. *J Clin Periodontol*, 2009. 36(10): p. 850-6.
92. De Keersmaecker SC., Verhoeven TL., et al., Strong antimicrobial activity of *Lactobacillus rhamnosus* GG against *Salmonella typhimurium* is due to accumulation of lactic acid. *FEMS Microbiol Lett*. 2006; 259(1): p. 89-96.
93. Barefoot SF., Klaenhammer TR., Purification and characterization of the *Lactobacillus acidophilus* bacteriocin lactacin B. *Antimicrob. Agents Chemother*, 1984. 26(3): p. 328-34.
94. Silva M., Jacobus NV., et al., Antimicrobial substance from human *Lactobacillus* strain. *Antimicro Ag and Chemother*, 1987. 31(8): p. 1231-3.
95. Ishikawa H., Aiba Y., et al., Suppression of periodontal pathogenic bacteria by the administration of *Lactobacillus salivarius* T12711. *J Jap Soc Periodontol*, 2003. 45(1): p.105-12.
96. Khalighi A., Behdani R., et al., Probiotics: A comprehensive review of their classification, mode of action and role in human nutrition. *Probiotics and Prebiotics in Human Nutrition and Health*. 2016.

97. Ahrne S., Nobaek S., et al. The normal *Lactobacillus* flora of healthy human rectal and oral mucosa. *J Appl Microbiol*, 1998. 85(1): p. 88-94.
98. Maukonen J., Mätto J., et al., Intra-individual diversity and similarity of salivary and faecal microbiota. *J Med Microbiol*, 2008. 57(12): p.1560-8.
99. Colloca ME., Ahumada MC., et al., Nader-Macias ME. Surface properties of lactobacilli isolated from healthy subjects. *Oral Dis*, 2000. 6(4): p. 227-33.
100. Simark-Mattsson C., Emilson CG., et al., *Lactobacillus*-mediated interference of mutans *Streptococci* in caries-free vs. caries-active subjects. *Eur J Oral Sci*, 2007.115(4): p. 308-14.
101. Rotimi VO., Duerden BI., The development of the bacterial flora in normal neonates. *J Med Microbiol*, 1981. 14(1): p. 51-62.
102. Gueimonde M., Laitinen K., et al., Breast milk: a source of bifidobacteria for infant gut development and maturation? *Neonatology*, 2007. 92(1): p. 64-6.
103. Abrahamsson TR., Sinkiewicz G., et al., Probiotic *Lactobacilli* in breast milk and infant stool in relation to oral intake during the first year of life. *J Pediatr Gastroenterol Nutr*, 2009. 49(3): p. 349-54.
104. Crociani F., Biavati B., et al., *Bifidobacterium inopinatum* sp. nov. and *Bifidobacterium denticolens* sp. nov., two new species isolated from human dental caries. *Int J Syst Bacteriol*, 1996. 46(2): p. 564-71.
105. Beighton D., Gilbert SC., et al., Isolation and identification of *bifidobacteria cesae* from human saliva. *Appl Environ Microbiol*, 2008. 74(20): p. 6457-60.
106. Metchnikoff E., Studier ofver människans natur försök till en optimistisk filosofi, bemyndigad ofvers. från tredje franska uppl. 3th Edition. Stockholm: Isaac Marcus' boktr. aktiebolag, 1906.
107. Köll-Klais P., Mandar R., et al., Oral *Lactobacilli* in chronic periodontitis and periodontal health: species composition and antimicrobial activity. *Oral Microbiol Immunol*, 2005, 20(6): p. 354-61.
108. Hojo K., Mizoguchi C., et al., Distribution of salivary *Lactobacillus* and *Bifidobacterium* species in periodontal health and disease. *Biosci Biotechnol Biochem*, 2007. 71(1): p.152-7.
109. Kragen H., The treatment of inflammatory affections of the oral mucosa with a lactic acid bacterial culture preparation. *Zahnärztl Welt*, 1954. 9(110): p. 306-8.
110. Talarico TL., Dobrogosz WJ., Chemical characterization of an antimicrobial substance produced by *Lactobacillus reuteri*. *Antimicrob Agents Chemother*, 1989. 33(5): p. 674-9.
111. Theodoro LH., Cláudio MM., et al., Effects of *Lactobacillus reuteri* as an adjunct to the treatment of periodontitis in smokers: randomised clinical trial. *Benef Microbes*, 2019. 10(4): P. 375-84.
112. Soares LG., De Carvalho EB., et al., Clinical effect of *Lactobacillus* on the treatment of severe periodontitis and halitosis: a double-blinded, placebo-controlled, randomized clinical trial. *Am J Dent*, 2019.32(1): p. 9-13.
113. Galofré M., Palao D., et al., Clinical and microbiological evaluation of the effect of *Lactobacillus reuteri* in the treatment of mucositis and periimplantitis: a triple-blind randomized clinical trial. *J Periodontal Res*, 2018. 53(3): p. 378-90.
114. Kang MS., Oh JS., et al., Inhibitory effect of *Lactobacillus reuteri* on periodontopathic and cariogenic bacteria. *J Microbiol*, 2011. 49(2): p. 193-9.
115. Iniesta M., Herrera D., et al., Probiotic effects of orally administered *Lactobacillus reuteri*-containing tablets on the subgingival and salivary microbiota in patients with gingivitis. A randomized clinical trial. *J Clin Periodontol*, 2012. 39(8): p. 736-44.
116. Krasse P., Carlsson B., et al., Decreased gum bleeding and reduced gingivitis by the probiotic *Lactobacillus reuteri*. *Swed Dent J*, 2006. 30(2): p.55-60.
117. Della Riccia DN., Bizzini F., et al., Anti-inflammatory effects of *Lactobacillus brevis* (CD2) on periodontal disease. *Oral Dis*, 2007.13(4): p. 376-85.
118. Twetman S., Derawi B., et al., Short-term effect of chewing gums containing probiotic *Lactobacillus reuteri* on the levels of inflammatory mediators in gingival crevicular fluid. *Acta Odontol Scand*, 2009. 67(1): p.19-24.
119. Teughels W., Newman MG., et al., Guiding periodontal pocket recolonization: a proof of concept. *J Dent Res*, 2007. 86(11): p.1078–82.
120. Nackaerts O., Jacobs R., et al., Replacement therapy for periodontitis: pilot radiographic evaluation in a dog model. *J Clin Periodontol*, 2008. 35(12): p. 1048–52.
121. Zhang YS., Yue K., et al., 3D bioprinting for tissue and organ fabrication. *Ann. Biomed. Eng*, 2017. 45(1): p.148–63.

122. 3D Bioprinting: Bioink selection guide. (2019). Retrieved from <https://www.sigmaaldrich.com/technical-documents/articles/materials-science/3d-bioprinting-bioinks.html>.
123. Intini C., Elviri L., et al., 3D-printed chitosan-based scaffolds: an *in vitro* study of human skin cell growth and an *in-vivo* wound healing evaluation in experimental diabetes in rats. *Carbohydr. Polym.* 2018. 199: p. 593–602.
124. Chen Y., Shen Y., et al., Osteogenic and angiogenic potentials of the cell-laden hydrogel/mussel-inspired calcium silicate complex hierarchical porous scaffold fabricated by 3D bioprinting. *Mater. Sci. Eng. C Mater. Biol. Appl.* 2018. 91: p. 679–87.
125. Rahman SU., Nagrath M., et al., Nanoscale and macroscale scaffolds with controlled-release polymeric systems for dental craniomaxillofacial tissue engineering. *Materials*, 2018. 11(8): p. 1478.
126. Lee V., Singh G., et al., Design and fabrication of human skin by three-dimensional bioprinting. *Tissue Eng. Part C Methods*, 2014. 20(6): p. 473–84.
127. Almela T., Al-Sahaf S., et al., 3D printed tissue engineered model for bone invasion of oral cancer. *Tissue Cell*, 2018. 52: p. 71–7.
128. Le Guéhennec L., Van hede D., et al., In vitro and in vivo biocompatibility of calcium-phosphate scaffold three-dimensional printed by stereolithography for bone regeneration. *J Biomed Mater Res*, 2020. 108A: p. 412–25.
129. Kim BS., Kwon YW., et al., 3D cell printing of in vitro stabilized skin model and in vivo pre-vascularized skin patch using tissue-specific extracellular matrix bioink: A step towards advanced skin tissue engineering. *Biomaterials*, 2018. 168: p. 38-53.
130. Kolesky D., Homan K., et al., Three-dimensional bioprinting of thick vascularized tissues. *Proc Natl Acad Sci USA*, 2016. 113(12): p. 3179-84.
131. Vijayavenkataraman S., Kannan S., et al., 3D-Printed PCL/PPy conductive scaffolds as three-dimensional porous nerve guide conduits (NGCs) for peripheral nerve injury repair. *Front. Bioeng. Biotechnol.* 2019. 7: p. 266.
132. Hong N., Yang GH., et al., 3D bioprinting and its in vivo applications. *J Biomed Mater Res Part B*, 2018. 106(1): p. 444–59.
133. Image adapted from: <https://www.zmescience.com/research/inventions/3d-printing-heart-15042019>
134. Prendergast ME., Solorzano RD., et al., Bioinks for biofabrication: current state and future perspectives. *J. 3D Print. Med.* 2017. 1(1): p. 49–62.
135. Malda J., Visser J., et al., 25th Anniversary article: engineering hydrogels for biofabrication. *Adv. Mater.* 2013. 25(36): p. 5011-28.
136. Gasperini L., Mano JF., et al., Natural polymers for the microencapsulation of cells. *J. R. Soc. Interface*, 2014. 11(100): p. 20140817.
137. Carrow JK., Keratitayanan P., et al., Polymers for bioprinting. In: *Essentials of 3D Biofabrication and Translation*. Academic Press, Winston Salem, 2015. p. 229–48.
138. Bertassoni LE., Cecconi M., et al., Hydrogel bioprinted microchannel networks for vascularization of tissue engineering constructs. *Lab Chip*, 2014. 14(13): p. 2202–11.
139. Blaeser A., Campos DFD., et al., Controlling shear stress in 3D bioprinting is a key factor to balance printing resolution and stem cell integrity. *Adv. Health. Mat.* 2016. 5(3): p. 326–33.
140. Bandyopadhyay A., Bose S., et al., 3D printing of biomaterials. *MRS Bull.* 2015. 40(2): p. 108–15.
141. Kundu J., Shim JH., et al., An additive manufacturing-based PCL-alginate-chondrocyte bioprinted scaffold for cartilage tissue engineering. *J. Tissue Eng. Regen. Med.* 2015. 9(11): p. 1286–97.
142. Chandrashekhara P., Minooei F., et al., Perspectives on existing and novel alternative intravaginal probiotic delivery methods in the context of bacterial vaginosis infection. *The AAPS Journal*, 2021. 23(3): p. 66.
143. Miller J., Stevens K., et al., Rapid casting of patterned vascular networks for perfusable engineered 3D tissues. *Nat. Mater.* 2012. 11(9): p. 768–74.
144. Gudapati H., Dey M., et al., A comprehensive review on droplet-based bioprinting: past, present and future. *Biomaterials*, 2016. 102: p. 20–42.
145. Kulseng B., Skjåk-Bræk G., et al., Transplantation of alginate microcapsules: generation of antibodies against alginates and encapsulated porcine islet-like cell clusters. *Transplantation*, 1999. 67(7): p. 978–84.
146. Moradali MF., Ghods S., et al., Alginate biosynthesis and biotechnological production. In *Alginates and their biomedical applications*. Springer, 2018. p. 1–25.

147. Chung JHY., Naficy S., et al., Bio-ink properties and printability for extrusion printing living cells. *Biomater. Sci*, 2013.1(7): p. 763–73.
148. Duan B., Hockaday L., et al., 3D bioprinting of heterogeneous aortic valve conduits with alginate/gelatin hydrogels. *J. Biomed. Mater. Res*, 2013. 101(5): p. 1255–64.
149. Ferris CJ., Gilmore K., et al., Bio-ink for on-demand printing of living cells. *Biomater. Sci*, 2013. 1(2): p. 224–30.
150. Axpe E., Oyen ML., Applications of alginate-based bioinks in 3D bioprinting. *Int J Mol Sci*, 2016. 17(12): p.1976.
151. Das D., Zhang S., et al., Synthesis and characterizations of alginate- α -tricalcium phosphate microparticle hybrid film with flexibility and high mechanical property as biomaterials. *Biomed Mater*, 2018. 13(2): p. 025008.
152. Skardal A., Atala A., et al., Biomaterials for integration with 3-D bioprinting. *Ann. Biomed. Eng*, 2015. 43(3): p.730–46.
153. Bertassoni LE., Cardoso JC., et al., Direct-write bioprinting of cell-laden methacrylated gelatin hydrogels. *Biofabrication*, 2014. 6(2): p.024105.
154. Pati F., Jang J., et al., Extrusion bioprinting, essentials of 3D biofabrication translation, 2015. p. 123-52.
155. Melchels FP., Domingos MA., et al., Additive manufacturing of tissues and organs. *Progress in Polymer Science*, 2012. 37(8):1079–104.
156. Wonhye L., Jason P., et al., Three-dimensional bioprinting of rat embryonic neural cells. *Neuroreport* 2009. 20(8):798–803.
157. Ozbolat IT., Yu Y., Bioprinting toward organ fabrication: challenges and future trends. *IEEE Transactions on Biomedical Engineering*, 2013. 60(3): p. 691–9.
158. Ferris CJ., Gilmore KJ., et al., Bioink for on-demand printing of living cells. *Biomaterials Science*, 2013. 1(2): p. 224–30.
159. Markstedt K., Mantas A., et al., 3D bioprinting human chondrocytes with nanocellulose alginate bioink for cartilage tissue engineering applications. *Biomacromolecules*, 2015. 16(5): p. 1489–96.
160. Xu C., Zhang M., et al., Study of droplet formation process during drop-on-demand ink jetting of living cell-laden bioink. *Langmuir*, 2014. 30(30): p. 9130–8.
161. Tyler KM., Morgan B., et al., A 3D bioprinted complex structure for engineering the muscle–tendon unit. *Biofabrication*, 2015. 7(3): p. 035003.
162. Rod RJ., Maria JR., et al., Evolution of bioinks and additive manufacturing technologies for 3D Bioprinting. *ACS Biomater. Sci. Eng*, 2016. 2(10): p. 1662–78.
163. Valot L., Martinez J., et al., Chemical insights into bioinks for 3D printing. *Chem. Soc. Rev.*, 2019. 48(15): p. 4049-86.
164. T Okamoto, T Suzuki , et al., Microarray fabrication with covalent attachment of DNA using bubble jet technology. *Nat. Biotechnol*, 2000. 18(4): p. 438–41.
165. Parsa S., Gupta M., et al., Effects of surfactant and gentle agitation on inkjet dispensing of living cells. *Biofabrication*, 2010. 2(2): p. 025003.
166. Chang R., Nam J., et al., Effects of dispensing pressure and nozzle diameter on cell survival from solid freeform fabrication-based direct cell writing. *Tissue Eng., Part A*, 2008. 14(1): p. 41–8.
167. Hopp B., Smausz T., et al., Survival and proliferative ability of various living cell types after laser-induced forward transfer. *Tissue Eng*. 2005, 11(11–12):p. 1817–23.
168. Kitty AM., Nuno R., et al., Ink-Jet printing of wax-based alumina suspensions. *J. Am. Ceram. Soc*, 2001. 84 (11): p. 2514–20.
169. Xu T., Binder KW., et al., Hybrid printing of mechanically and biologically improved constructs for cartilage tissue engineering applications. *Biofabrication*, 2013. 5(1): p. 015001.
170. Phillippi JA., Miller E., et al., Microenvironments engineered by inkjet bioprinting spatially direct adult stem cells toward muscle- and bone-like subpopulations. *Stem Cells*, 2008. 26(1): p. 127–34.
171. Ringeisen B., Othon CM., et al., Jetbased methods to print living cells. *Biotechnology journal*, 2006. 1(9): p. 930–48.
172. A Ovsianikov, M Gruene, et al., Laser printing of cells into 3D scaffolds. *Biofabrication*, 2010. 2(1): p. 014104.
173. Lothar K., Andrea D., et al., Skin tissue generation by laser cell printing. *Biotechnology and bioengineering*, 2012. 109(7): p. 1855–63.

174. Arcaute K., Mann B., et al., Stereolithography of three-dimensional bioactive poly (ethylene glycol) constructs with encapsulated cells. *Ann. Biomed. Eng.*, 2006. 34(9): p. 1429–41.
175. CE. Moffatt-Jauregui, B. Robinson, et al., Establishment and characterization of a telomerase immortalized human gingival epithelial cell line. *J Periodontal Res*, 2013. 48(6): p. 713-21.
176. Image adapted from: <https://3dprint.com/wp-content/uploads/2018/09/unnamed-40.jpg>.
177. Desai H., Mahmoud MY., et al., Assessment of Caf A targeted BAR-encapsulated nanoparticles against oral biofilms. *Pharmaceutics*, 2020.12(9): p. 835.
178. Kalia P., Jain A., et al., Peptide-modified nanoparticles inhibit formation of *Porphyromonas gingivalis* biofilms with *Streptococcus gordonii*. *Int J Nanomedicine*, 2017. 12: p. 4553-62
179. Twana MMW., Wing ML., et al., Chitosan and its derivatives for application in mucoadhesive drug delivery systems. *Polymers (Basel)*, 2018. 10(3): p. 267.
180. Toshiharu A., Hajishengallis G., Optimization of the ligature-induced periodontitis model in mice. *Journal of Immunological Methods*, 2013. 394(1-2): p. 49-54.
181. Graves DT, Fine D., et al., The use of rodent models to investigate host-bacteria interactions related to periodontal diseases. *Journal of clinical periodontology*, 2008. 35(2): p. 89-105.
182. Helieh S. Oz, David AP., Animal models for periodontal disease. *Jof biomed biotechnol*, 2011. 2011: p. 754857
183. MM Bezerra, V de Lima, et al., Selective cyclooxygenase-2 inhibition prevents alveolar bone loss in experimental periodontitis in rats. *J Periodontol*, 2000. 71(6): 1009-14.
184. Chung HL., Salomon A., Morphometric, histo-morphometric, and microcomputed tomographic analysis of periodontal inflammatory lesions in a murine model. *J Periodontol*, 2007. 78(6): p. 1120-28.
185. Baker PJ., Evans RT., et al., Oral infection with *Porphyromonas gingivalis* and induced alveolar bone loss in immunocompetent and severe combined immunodeficient mice. *Arch Oral Biol*, 1994. 39(12): p. 1035-40.
186. Hart GT., Shaffer DJ., et al., Quantitative gene expression profiling implicates genes for susceptibility and resistance to alveolar bone loss. *Infect Immun*, 2004. 72(8): p. 4471- 7.

CURRICULUM VITAE

Name: Jhanvi Patel

Education:

College of Dental Sciences and Research Centre,
Bachelor of Dental Surgery (B.D.S)

2011-2016

Presentations:

IADR, July 2021

Poster: Development of 3D bioprinted scaffolds containing probiotics for Oral Delivery Applications.